Constraints on the vital effect in coccolithophore and dinoflagellate calcite by oxygen isotopic modification of seawater

Michaël Hermoso[1,*], Tristan J. Horner[1,2], Fabrice Minoletti[3,4], and Rosalind E.M. Rickaby[1]

[1] University of Oxford – Department of Earth Sciences. South Parks Road, Oxford OX1 3AN, United Kingdom.

[2] Woods Hole Oceanographic Institution – Department of Marine Chemistry and Geochemistry, Woods Hole, MA 02543, United States of America.

[3] UPMC Université Paris 06 – UMR 7193 ISTeP, 4 Place Jussieu, 75005 Paris, France.

[4] CNRS – UMR CNRS 7193 ISTeP, 4 Place Jussieu, 75005 Paris, France.

[*] Corresponding author. Email: Michael.Hermoso@earth.ox.ac.uk. Ph: +44 (0) 1865 272003.

ABSTRACT

In this study, we show that there are independent controls of $^{18}O/^{16}O$ and $^{13}C/^{12}C$ fractionation in coccolithophore and dinoflagellate calcite due to the contrasting kinetics of each isotope system. We demonstrate that the direction and magnitude of the oxygen isotope fractionation with respect to equilibrium is related to the balance between calcification rate and the replenishment of the internal pool of dissolved inorganic carbon (DIC). As such, in fast growing cells, such as those of *Emiliania huxleyi* and *Gephyrocapsa oceanica* (forming the so-called "heavy group"), calcification of the internal carbon pool occurs faster than complete isotopic re-adjustment of the internal DIC pool with H_2O molecules. Hence, coccoliths reflect the heavy oxygen isotope signature of the CO_2 overprinting the whole DIC pool. Conversely, in large and slow growing cells, such as *Coccolithus pelagicus* ssp. *braarudii,* complete re-equilibration is achieved due to limited influx of CO_2 leading to coccoliths that are precipitated in conditions close to isotopic equilibrium ("equilibrium group"). Species exhibiting the most negative oxygen isotope composition, such as *Calcidiscus leptoporus* ("light group"), precipitate coccolith under increased *p*H in the coccolith vesicle, as previously documented by the "carbonate ion effect". We suggest that, for the carbon isotope system, any observed deviation from isotopic equilibrium is only "apparent", as the carbon isotopic composition in coccolith calcite is controlled by a Rayleigh fractionation originating from preferential incorporation of ^{12}C into organic matter. Therefore, species with low PIC/POC ratios as *E. huxleyi* and *G. oceanica* are shifted towards positive carbon isotope values as a result of predominant carbon fixation into the organic matter. By contrast, cells with higher PIC/POC as *C. braarudii* and *C. leptoporu*s maintain, to some extent, the original negative isotopic composition of the CO_2. The calcareous dinoflagellate *Thoracosphaera heimii* exhibits different behaviour for both isotopic systems, in particular

with respect to its very negative carbon isotope composition, owing to coeval intra and extracellular biomineralisation in this group. In this study, we also investigate the sensitivity of $^{18}O/^{16}O$ fractionation to varying ambient oxygen isotope composition of the medium for inorganic, coccolithophore, and dinoflagellate calcite precipitated under controlled laboratory conditions. The varying responses of different taxa to increased oxygen isotope composition of the growth medium may point to a potential bias in sea surface temperature reconstructions that are based on the oxygen isotopic compositions of sedimentary calcite, especially during times of changing seawater oxygen isotopic composition. Overall, this study represent an important step towards establishing a mechanistic understanding of the "vital effect" in coccolith and dinoflagellate calcite, and provides valuable information for interpreting the geochemistry of the calcareous nannofossils in the sedimentary record, at both monospecific and interspecies levels.

1. INTRODUCTION

Understanding how stable isotopes in biogenic calcite reflect the physico-chemical composition of the environment is crucial for interpreting the sedimentary record. One of the most prominent components of pelagic sediments since the Jurassic is the coccoliths, polycrystalline structures of $CaCO_3$ that are produced by the coccolithophores (Haptophyta). As coccoliths are produced intracellularly, their geochemical signals are prone to physiological imprinting, a phenomenon referred to as the "vital effect". The concept of vital effects embraces a wide range of thermodynamic and physiological processes that induce offsets between inorganic and biogenic $CaCO_3$ (Weiner and Dove, 2003). The clearest evidence of the vital effect imparted by coccolithophores on coccolith calcite is the differential isotopic fractionation seen between species. Indeed, a wide range of $\delta^{18}O$ and $\delta^{13}C$

values have been found in coccolith calcite in both culture experiments (Dudley et al., 1986; Ziveri et al., 2003; Rickaby et al., 2010) and from monotaxic coccolith or size restricted assemblages isolated from sediments (Minoletti et al., 2009; Bolton et al., 2012; Bolton and Stoll, 2013). Dudley et al. (1986) grouped the coccolithophores on the basis of their $\delta^{18}O$ signatures relative to equilibrium conditions and defined: an isotopically "heavy group" and an isotopically "light group". The first group comprises the small cells and coccoliths of *Emiliania huxleyi* and *Gephyrocapsa oceanica*, whereas the second comprises the large cells such as *Coccolithus braarudii* and *Calcidiscus leptoporus*. For a given temperature of calcification, the maximum interspecies offset in $\delta^{18}O$ has been reported to be as high as 5 ‰ (Dudley et al., 1986). Such an array of $\delta^{18}O$ values in coccolithophores grown under comparable conditions is problematic for reconstructing robust sea surface temperatures from any mixed assemblage of coccolith calcite. Interspecies differences correspond, at face value, to a difference in ambient temperature estimates of up to 20 °C. Further work is threfore needed to understand the vital effect in coccoliths in order to fully exploit the sedimentary archive, as these nannofossils often represent the greatest fraction of pelagic sediments (Broecker and Clark, 2009).

Indeed, the causes of biologically induced isotopic fractionation in coccolith calcite are still poorly constrained. It is likely that transmembranal transport of DIC and the nature of the substrate used for calcification are responsible for a combination of kinetic and equilibrium effects, respectively. The former (kinetic effects) are thought to be a consequence of a suite of strategies, as active CO_2 and HCO_3^- uptake, termed CO_2 Concentrating Mechanisms (CCMs) that phytoplankton cells use to boost the concentration of CO_2 in the cell (see review of Giordano et al., 2005). From the ancient geological record, it has been shown that coccoliths record isotopic signatures close to that of inorganic precipitates in the Early Jurassic (Hermoso et al., 2009). Further, there were no differential vital effects among

different sized coccoliths analysed from the Late Palaeocene until the appearance of interspecies offsets since the Late Miocene interval (Stoll, 2005; Bolton and Stoll, 2013); which has lead to the suggestion that induction of CCMs in some coccolith species in response to declining ambient carbon dioxide may be responsible for much of the vital effect (Bolton et al., 2012). Culture experiments further suggest that the vital effect is dependent on external carbon availability (Rickaby et al., 2010).

There have been a number of studies that have investigated the temperature dependence on $^{18}O/^{16}O$ fractionation in $CaCO_3$. However, the influence of the isotopic composition of the growth medium or of seawater on the magnitude of stable isotope fractionation, in the absence of study, has been assumed to be negligible. In the present study, we investigate how changing oxygen isotope composition of the culturing medium affects the magnitude of $^{13}C/^{12}C$ and $^{18}O/^{16}O$ fractionation for a wide range of coccolithophore species *Emiliania huxleyi*, *Gephyrocapsa oceanica*, *Coccolithus pelagicus* ssp. *braarudii*, and *Calcidiscus leptoporus*, and for the calcareous dinoflagellate *Thoracosphaera heimii* (Table 1). Both groups (coccolithophores and dinoflagellates) have distinct modes of biomineralisation with a probably less controlled environment of mineralisation for the latter (Zonneveld et al., 2007). We have also conducted several laboratory precipitation experiments of calcite under the same ambient conditions as the cultures, which serve as an inorganic (abiogenic) control in order to acquire a mechanistic understanding of the equilibrium and kinetic processes responsible for vital effects. A direct outcome of our work is to provide constraints on the use of oxygen isotope compositions in coccolith and dinoflagellate calcite for palaeotemperature reconstruction. Determining how the $\delta^{18}O$ of seawater ($\delta^{18}O_w$) affects the isotopic fractionation during precipitation is fundamental to the deduction of reliable temperature from calcite $\delta^{18}O$ ($\delta^{18}O_c$), when investigating periods of contrasting $\delta^{18}O_w$.

2. METHODS

2.1. Algal cultures

Laboratory cultures of monoclonal strains of calcifying phytoplankters were performed at the Oxford Biogeochemistry Laboratory in January 2012. All the experiments were undertaken at 15 °C (± 0.2 °C). Experiments were conducted in 200 mL polystyrene Thermo Scientific NUNC® sterile flasks with 50 mL headspace. The basis of the culturing medium consisted of natural aged seawater obtained from the Marine Biologist Association, Plymouth (UK). To change the $\delta^{18}O_w$ of the natural batch of seawater (0.69 ‰ [V-SMOW]), addition of a DIC free (argon flushed) solution of water containing 97.2 % ^{18}O; 0.5 % ^{17}O; and 2.3 ‰ ^{16}O atoms (Euriso-top Inc. Saclay, France) was used to reach the targeted $\delta^{18}O_w$ under a range of values between 0 ‰ and 75 ‰ (relative to V-SMOW). Although this range of oxygen isotope composition of seawater is very large, it provides more precise quantification of the $\delta^{18}O_c$ /$\delta^{18}O_w$ relationship than if studying the more restricted range of natural changes documented for the last 65 Myrs (Zachos et al., 2001). Each batch of $\delta^{18}O$-modified seawater was left for 10 days at 4 °C to allow re-equilibration of the oxygen isotopes in the $H_2O - CO_{2\,(aq)} - HCO_3^- - CO_3^{2-}$ system, and subsequently bubbled for 24 hours with air to equilibrate the $\delta^{13}C$ of the DIC with the atmosphere. Addition of nitrate, phosphate, trace metals, EDTA was that of the K/2 medium (Keller et al., 1987) and the vitamins that of the f/2 medium (Guillard, 1975). The medium *p*H was increased by addition of 0.2 M NaOH until *p*H 8.2 was obtained. The growth medium was finally sterilised by steri-filtration (0.22 μm) using disposable Millipore® Stericup devices. The pCO_2 of the bubbled air determined by a LI-COR Analyser, and the imposed *p*H enable calculation of the initial

concentration of DIC on the order of 2.5 mM using the CO2calc software (Robbins et al., 2010).

In the incubator, light was supplied by fluorescent bulbs with a light/dark cycle of 14/10 hours. During the illuminated period, irradiance was measured at ~ 250 μmol photons / m^2 / s. At the end of the experiments, cells were harvested by centrifugation when the density reached ~ 10,000 for *E. huxleyi* and between 5,000 and 6,000 cells per mL for all other taxa. An aliquot of each batch of $\delta^{18}O$-modified water sample was taken and kept at 4 °C for further measurement of $\delta^{18}O_w$ and $\delta^{13}C$ of DIC at the beginning of the experiment.

2.2. Determination of growth rate

Growth rates were calculated by measuring cell density (cells / mL) using a Beckman Coulter Counter Series Z2 apparatus. A volume of 2 mL of culture was diluted with 8 mL ISOTON II diluent and measured using a 100 μm aperture tube. Typical growth rates for each species (noted μ) were calculated during the early exponential phase of the algal population growth using the formula:

$$\mu = [\ln(c_{final}) - \ln(c_{initial})] / Nb\_day \quad \text{(Eq. 1)}$$

where c is the concentration of cells, and Nb_day is the number of days elapsed between the two measurements made one hour after the beginning of the light period.

For each species, no significant difference in μ was observed between batches with $\delta^{18}O$-modified values. Coccosphere diameters (spherical equivalent) were measured using the mode of the Gaussian size distribution provided by the Coulter Counter apparatus calibrated using 10.16 μm diameter latex beads provided by Beckman Coulter.

2.3. Measurement of PIC/POC ratio

Measurements of the particulate inorganic carbon (PIC) and particulate organic carbon (POC) of culture residues were made using a Rock Eval 6 pyrolyser (Vinci Technologies) at Oxford University. As the aliquot required to produce a reliable PIC/POC ratio (~ 5 mg) is much higher than obtained in our modified $\delta^{18}O$ experiments, larger batches were grown in parallel at the same temperature and light irradiance and were subjected to PIC/POC analyses. We assume that the larger experiments performed in strictly parallel conditions than the $\delta^{18}O$-modified cultures are representative of these smaller cultures, as evidenced by near-identical growth rates. Nevertheless, the PIC/POC ratios provided here have to be regarded as estimates. Indeed, in the following account, we do not use these figures for calculating the partitioning of carbon between photosynthesis and calcification. Our PIC/POC are in the same order as previously documented ratios (Langer et al., 2006, 2009; Van der Waal et al., 2013). Rinsed and dried culture residues were loaded into pre-combusted crucibles, and successively pyrolised and thermo-oxidised from 100 to 850 °C in the instrument. CO and CO_2 gases were measured by FID / Infrared cells, and their abundance converted into organic versus mineral-bound carbon depending on their elution time within the running temperature-O_2 cycles (see Behar et al., 2001 for further details).

2.4. Inorganic calcite precipitation

Calcium carbonate precipitation was performed using an ^{18}O-unmodified artificial seawater matrix spiked with the same ^{18}O-enriched isotope solution, as that used for the cultures (final targeted isotopic values: 1; 5; 10; 25; 50 and 75 ‰ rel. V-SMOW). The media

contained the following salts: 30 g NaCl; 4.1 g Na_2SO_4; 0.84 g $NaHCO_3$; 0.7 g KCl; and 0.46 g H_3BO_3 (per L). The *p*H of the solutions was brought to 8.2 by addition of 1M NaOH. Each experiment was conducted in 500 mL polycarbonate vessels that were submerged in a 100 L thermostatically-controlled water bath at 15 °C. Saturation state with respect to $CaCO_3$ and subsequent precipitation was achieved by adding a solution of 1M $CaCl_2$ using a syringe-pump system. Five millilitres of the $CaCl_2$ solution was added to each flask and left for 24 hours. Calcite precipitates were gathered by vacuum filtration on 0.8 μm polycarbonate membrane filters. After rinsing the residues with neutralised deionised water, approximately 30 μg of powder (pure calcite checked by XRD) were subsequently analysed for $\delta^{13}C$ and $\delta^{18}O$. Unfortunately, we were not able to measure a final dried mass of produced calcite, precluding calculation of a precipitation rate. This method consisting of $CaCl_2$ addition into a DIC-rich solution was chosen to ensure all the DIC species and the H_2O molecules were in permanent thermodynamic equilibrium.

2.5. Isotopic measurements

2.5.1. Water samples

The $\delta^{18}O_w$ of the culturing media was measured from the isotopic determination of the CO_2 in the headspace of the culturing vessel, equilibrated with a 0.5 mL aliquot in Exetainer tubes using Gas Bench II coupled to a Delta V Advantage mass spectrometer at the University of Oxford. Three international water standards (IA-RO53, IA-RO54, and IA-RO55; $\delta^{18}O$ = –10.18 ‰, +0.56 ‰, and +108.63 ‰ [V-SMOW], respectively) were run to perform a three-point external calibration for the raw isotopic results. Reproducibility of replicated results ($\delta^{18}O_w$ expressed in V-SMOW) was usually better than 0.2 ‰ for $\delta^{18}O$ of the media.

Measurement of initial $\delta^{13}C_{DIC}$ of medium of both precipitation and culture experiments was performed at the Godwin Laboratory for Palaeoclimate Research, Cambridge (UK) using a Thermo Gas Bench attached to a Delta V Mass Spectrometer. Three drops of orthophosphoric acid (100 %) were preloaded into a reaction vial, which was capped, sealed and the headspace flushed with helium gas. Approximately 1.5 mL of sterile medium sample was injected into the vial through the butyl rubber septa using a syringe and left to react for one hour. The sample tubes were transferred to the Gas Bench and CTC CombiPal Autosampler and the resulting CO_2 in the headspace analysed using a Thermo Delta V Mass Spectrometer. A series of standards and reference samples distributed through out the run were used to calibrate to the international standard. Results expressed in the V-PDB scale have a reproducibility of better than 0.1 ‰.

2.5.2. Carbonate samples

Culture residues were measured for their carbon and oxygen isotope ratios ($\delta^{13}C_c$ and $\delta^{18}O_c$, respectively) using a VG Isogas Prism II mass spectrometer with an on-line VG Isocarb at Oxford University. About 5 mg of homogenised samples were first cleaned using neutralised hydrogen peroxide (H_2O_2) and dried at 60 °C. In the instrument, samples were reacted with purified orthophosphoric acid at 90 °C. Calibration to V-PDB standard via NBS-19 is made daily using the Oxford in-house (NOCZ) Carrara marble standard ($\delta^{13}C$ = 2.09 ‰ [V-PDB], $\delta^{18}O$ = –1.86 ‰ [V-PDB]). Reproducibility of replicated standards is usually better than 0.1 ‰ for $\delta^{13}C$ and $\delta^{18}O$.

2.5.3. Expression of the results

Fractionation factors can be expressed by the difference between the composition of the carbonate in V-PDB ($\delta^{18}O_c$) and that of the medium in V-SMOW ($\delta^{18}O_w$) using the "δ – δ" notation. Results can also be compared to inorganic precipitation or calculated equilibrium conditions. In this study we use the isotopic composition of our inorganic calcite precipitates as our reference. Furthermore, we plotted the calculated equilibrium of Kim and O'Neil (1997) corrected by a factor of 0.4 ‰ to the intersect of their equation to account for precipitation at *p*H 8.2 rather than 7.8 (Eq. 2; see Candelier et al., 2013). The oxygen isotope composition of "equilibrium" calcite ($\delta^{18}O_{eq}$) for each water sample is then calculated using measured $\delta^{18}O_w$ and for a temperature of calcification of 15 °C.

$$\delta^{18}O_{eq\,[V\text{-}PDB]} = \delta^{18}O_{w\,[V\text{-}SMOW]} + [\,(0.0009 \times T^2) - (0.2468 \times T) + 3.0734)\,] \qquad \text{(Eq. 2)}$$

To obtain the carbon isotope composition of equilibrium calcite ($\delta^{13}C_{eq}$), we used the formula by Romanek et al. (1992) with the assumption that $\delta^{13}C_{DIC} \approx \delta^{13}C_{bicarbonate}$ at *p*H 8.2:

$$\delta^{13}C_{eq} = \delta^{13}C_{DIC} + 1 \qquad \text{(Eq. 3)}$$

The quantification of the biologically induced fractionation ("Vital Effect") can been calculated as the residual between the isotopic composition of the biogenic calcite and that of equilibrium inorganic calcite for both oxygen and carbon systems.

$$\text{"Vital Effect"}_{[V\text{-}PDB]} = \delta_{c\,[V\text{-}PDB]} - \delta_{eq\,[V\text{-}PDB]} \qquad \text{(Eq. 4)}$$

3. RESULTS

3.1. DIC and inorganically precipitated calcite isotopic compositions

3.1.1. Oxygen isotope results

We observe a robust linear relationship between $\delta^{18}O_w$ and $\delta^{18}O_c$ of inorganically precipitated calcite ($r^2 > 0.98$; Fig. 1a; Table 2). We determined a slope for $\delta^{18}O_w$ / $\delta^{18}O_c$ relationship of 0.98 (± 0.02 ‰), which is very close to the expected value of 1. A 1:1 correlation in the line shown in Fig. 1a would mean no change in $^{18}O/^{16}O$ fractionation with increased $\delta^{18}O_w$. This slight difference is attributable to the abundance of ^{17}O in the spiking solution (0.5 %). This concentration, which is significantly higher than in natural seawater, led to a higher "^{17}O artefact" in our ^{18}O enriched experiments (Santrock et al., 1985). This is because $\delta^{18}O$ of seawater or carbonate is meant to reflect the relative abundance of ^{18}O versus ^{16}O atoms, but the mass-spectrometric determination of this ratio uses the abundance of ^{17}O. This means that for a given $^{18}O/^{16}O$ ratio, an increased proportion of ^{17}O leads to a higher ^{17}O interference on isotopic determination of released CO_2 in the mass spectrometer, and a lower $\delta^{18}O$ ratio is measured. Nevertheless, the linear relationship between the isotopic composition of the medium and that of inorganic calcite allows us to use this "abiotic result" (the 1.00:0.98 correlation in Fig. 1a) as a reference from which the ^{17}O artefact is removed. In the following account, any isotopic offsets between coccolith calcite and our inorganic reference with changed $\delta^{18}O_w$ may be regarded as a consequence of changing vital effects. Lastly, it is worth noting that the $\delta^{18}O_c$ in our experiments is very close to the equilibrium calcite proposed by the Kim and O'Neil (1997) equation at 15 °C (Eq. 2).

3.1.2. Carbon isotope composition

The co-addition of ^{17}O in the medium also has an effect on the determination of the $^{45}CO_2/^{44}CO_2$ and $^{46}CO_2/^{44}CO_2$, and hence on $\delta^{13}C_{DIC}$ and $\delta^{13}C_c$ (Santrock et al., 1985; Brand et al., 2010). As a consequence, without addition of ^{12}C or ^{13}C in the spiking solution, we observe a decrease in both $\delta^{13}C_{DIC}$ and $\delta^{13}C_c$ with increasing $\delta^{18}O_w$ values due to an increase in ^{17}O concentrations (Fig. 1b). In our data, the maximum $\delta^{13}C_c$ offset on the range of measured $\delta^{18}O_w$ is significant and in the order of 2.5 ‰ (Fig. 2b). The $\delta^{13}C_c$ / $\delta^{18}O_w$ and $\delta^{13}C_{DIC}$/ $\delta^{18}O_w$ curves are strikingly linear ($r^2 = 0.98$) and parallel with a constant offset of 1 ‰, which is the predicted magnitude of ^{13}C fractionation in inorganic calcite (Romanek et al., 1992; Eq. 3). Quantitatively, the amplitude of the combined effect of ^{18}O and ^{17}O addition in inorganic $^{13}C/^{12}C$ fractionation can be assessed by the slope of the $\delta^{18}O_w$ / $\delta^{13}C_c$ linear relationship (Fig. 1b). Increasing the $\delta^{18}O_w$ of 1 ‰ results in a decrease of 0.03 ‰ in the $\delta^{13}C_{DIC}$ and similarly that of inorganically precipitated calcite.

3.2. Fractionation in biogenic calcite under unmodified $\delta^{18}O_w$ conditions

First, we examine the amplitude of the vital effect (sensu Eq. 4) from the isotopic composition of biogenic calcite grown in unmodified culture media (natural seawater; $\delta^{18}O_w$ = 0.69 ‰ [V-SMOW]), *i.e.* the intercept on Fig. 3a. Second, we calculate the sensitivity of the vital effect to the modification of the isotopic composition of the media via the slopes of $\delta^{18}O_c$ / $\delta^{18}O_w$ and $\delta^{13}C_c$ / $\delta^{18}O_w$ for each species in response to ^{18}O addition. The results are expressed as offsets from our inorganically precipitated calcite.

3.2.1. Oxygen isotope composition

The fast growing and relatively small taxa *E. huxleyi* and *G. oceanica* both fractionate oxygen isotopes towards heavy (high $\delta^{18}O$) values compared with predicted equilibrium (Table 3; Fig. 2a). The mean departure from inorganic calcite for these two taxa is 2.56 ‰ (± 0.08 ‰) and 1.27 ‰ (± 0.01 ‰) respectively. By contrast, *T. heimii* and *C. leptoporus* precipitate calcite with lower $\delta^{18}O$ signatures relative to equilibrium values, –0.99 ‰ (± 0.31 ‰) and –1.31 ‰ (± 0.04‰), respectively. *C. braarudii* appears to precipitate in near-equilibrium conditions in our study, –0.24 ‰ (± 0.17 ‰) from equilibrium calcite.

3.2.2. Carbon isotope composition

Emiliania huxleyi, whose composition is offset by 0.97 ‰ (± 0.01 ‰) with respect to inorganic reference, is the only species that exhibits more positive $\delta^{13}C_c$ than equilibrium calcite (Fig. 2b). *G. oceanica* is relatively close to the inorganic equilibrium (–0.28 ‰; ± 0.11 ‰). These two taxa are characterised by relatively low PIC/POC ratios < 1 (Table 1). Coccolithophores characterised by larger cells, lower division rates, and higher PIC/POC ratios (Table 1) show significantly lighter $\delta^{13}C$ compositions (*C. braarudii*: –1.56 ‰; ± 0.03 ‰; *C. leptoporus*: –3.32 ‰; ± 0.04‰). The dinoflagellate *T. heimii* has the most negative $\delta^{13}C_c$, equivalent to a –6.66 ‰ (± 0.04 ‰) offset from the inorganic reference.

3.3. Change in oxygen and carbon isotopic composition with increasing $\delta^{18}O_w$

3.3.1. Oxygen isotope composition

Slopes of ($\delta^{18}O_c - \delta^{18}O_w$) versus $\delta^{18}O_w$ significantly differ between species (Fig. 3a). The slope for *G. oceanica,* approximates a horizontal line close to the inorganically-

precipitated calcite line. The slopes in $^{18}O/^{16}O$ fractionation with increasing $\delta^{18}O_w$ appear to be parallel for *E. huxleyi*, *C. braarudii, and T. heimii* (Fig. 3a) with higher sensitivities to ^{18}O addition, as indicated by steeper slopes compared to *G. oceanica*. The largest change in fractionation factors is seen for *C. leptoporus*, which shows a decrease of approximately –13 ‰ in $\delta^{18}O$ between unmodified medium and the heaviest $\delta^{18}O_w$ of ~ +75 ‰. The results show that the reduction in the fractionation factor in response to ^{18}O addition appears to be most pronounced for species that have a more negative oxygen isotope composition under isotopically unmodified growth medium, as *C. leptoporus* (Fig. 4).

3.3.2. Carbon isotope composition

The typical slope of $\delta^{13}C_c$ change is within 0.8 ‰ for all species. *E. huxleyi* is the species that shows the most significant departure from the expected $\delta^{13}C_c$ / $\delta^{18}O_w$ line deduced from inorganic calcite (Fig. 3b). Conversely, the $\delta^{13}C_c$ of *T. heimii* increases with increasing $\delta^{18}O_w$ (Fig. 3b). However, for all the taxa including *E. huxleyi*, changes in the slopes are close to the uncertainty of combined $\delta^{13}C_{DIC}$ and $\delta^{13}C_c$ uncertainties (propagated slope uncertainty less than 0.5 ‰). Hence, we are not able to statistically demonstrate an effect on $^{13}C/^{12}C$ fractionation with increasing $\delta^{18}O_w$ for any taxon.

4. DISCUSSION

4.1. Modulation of apparent $^{18}O/^{16}O$ fractionation and dynamics of intracellular DIC

4.1.1. Mechanism for changing the magnitude of $^{18}O/^{16}O$ fractionation with increased $\delta^{18}O_w$

For our inorganically precipitated calcites, the lack of a change in $^{18}O/^{16}O$ fractionation is explained by the absence of modification in the magnitude of the kinetic effect occurring during precipitation. This constancy indicates that the $^{16}O/^{18}O$ discrimination is not dependent on $\delta^{18}O_w$ in abiogenic systems in which the DIC species and H_2O in solution are in thermodynamic equilibrium. By contrast, the addition of ^{18}O atoms in the growth medium seems to lower the magnitude of the kinetic fractionation in coccolith and dinoflagellate calcite, but this process is only apparent. Indeed, the "nature" of the fractionation process is unchanged: higher abundance of ^{18}O makes the preference for the light isotope larger relative to the isotopically heavier medium. As a result, immediately after transmembrane diffusion or uptake, the oxygen isotopes in the ambient DIC are less in equilibrium with H_2O in high $\delta^{18}O_w$ than in unmodified conditions. Indeed, our data show that there is a greater selection for the light isotopes in heavier $\delta^{18}O_w$ than in normal $\delta^{18}O_w$ of ~ 0 ‰. In solution, the time required to (re)-equilibrate the oxygen isotope of the H_2O – DIC system is of the order of 12 hours at 15 °C (Usdowski et al., 1991; Zeebe and Wolf-Gladrow, 2001; Beck et al., 2005; Zeebe, 2009; Rollion-Bard et al., 2011; Watkins et al., 2013). Hence, interspecific differences in apparent $^{18}O/^{16}O$ fractionation are set by the balance between oxygen isotope re-equilibration versus calcification processes. Species that erase the induced change in ^{18}O fractionation created by ^{18}O atom addition in the medium are those for which the internal carbon pool remains relatively longer in the cell before being mineralised. This change in the magnitude in apparent fractionation thus gives us the opportunity to examine how oxygen isotope disequilibria are transcribed (or not) into biogenic calcite, which can be interpreted in terms of the DIC "residence time" within cells.

4.1.2. Species-specific responses

For *G. oceanica*, the rather limited record of change in kinetic fractionation would indicate that this relatively fast growing and medium-sized cell has the lowest overturning rate of DIC that can be defined by the assimilation versus utilisation of DIC (replenishment rate). Indeed, in this species, the DIC has time to reach almost complete re-equilibration inside the cell before it is incorporated into calcite. The lack of external carbonic anhydrase for this species (Nimer et al., 1999), and its relatively bigger cell size may confirm a slow DIC supply or uptake compared to *E. huxleyi*. On the other hand, *C. leptoporus* is the species for which minimum isotopic re-equilibration is seen, suggesting that this cell has a relatively faster overturning rate of the intracellular DIC pool. In *C. leptoporus*, this extreme isotopic response would either indicate a relatively high DIC supply rate, which is unlikely considering slow growth rate, or fast mineralisation of the carbon pool, which is more likely regarding its high PIC (coccolith) production (Langer et al., 2006; Table 1). The nature of DIC acquisition and operating CCMs for species still have to be fully investigated.

Coccolithus braarudii relies on CO_2 for its source of carbon due to the lack of efficient CCMs (Nimer et al., 1999; Rickaby et al., 2010; Hermoso et al., 2013). Comparable slopes in change in apparent fractionation between *E. huxleyi* and *C. braarudii* may indicate that the two species, albeit characterised by very distinct growth rates, have comparable overturning rate of the DIC in the cells. However, a difference related to distinct PIC/POC ratio may modulate the isotopic effect seen by the calcite. Indeed significantly higher PIC/POC ratios measured for *C. braarudii* compared to *E. huxleyi* may change the residence time of DIC within the cell. As our experimental setup only takes into account the ambient DIC partitioned into calcification, similar response for two contrasting taxa may be a bias due to distinct carbon fixation by calcification and photosynthesis. This point may explain why *E. huxleyi* appears to be an outlier in the overall good correlation between oxygen fractionation in

unmodified medium and the gradient in decreased fractionation with ^{18}O addition in the medium shown in Fig. 4.

The calcareous dinoflagellate *Thoracosphaera heimii* has a $\delta^{18}O_c$ composition close to that of *C. leptoporus* under unmodified $\delta^{18}O_w$ conditions. Both species show, however, significantly different slopes in our ^{18}O addition experiments (Fig. 3A). The physiology of the dinoflagellate *T. heimii* and its mode of biocalcification differ from that happen in coccolithophores (Inouye and Pienaar, 1983). Two generations of calcification, one intracellular, the other extracellular take place in calcareous dinoflagellates that complicate the interpretation of the magnitude of the isotopic fractionation (Tangen et al., 1982; Inouye and Pienaar, 1983). Hence, the intermediate slope in ^{18}O fractionation under increased $\delta^{18}O_w$ for *T. heimii* located between *C. leptoporus* and the inorganic reference (Fig. 3A) is consistent with the idea that the calcite produced by this species represents a mixture of internal and external calcification.

4.2. Insights into the differential vital effects in coccolith calcite

This study also confirms the identification of two distinct groups of coccoliths based on the direction of $^{18}O/^{16}O$ fractionation with respect to equilibrium compositions in unmodified media. They are thus termed "heavy" (above inorganic calcite; Fig. 3a) and "light" (below inorganic calcite; Fig 3a) groups, as originally proposed by Dudley et al. (1986). Significant interspecific carbon isotope offsets also exist (Stoll and Ziveri, 2004; Fig. 3b). Table 4 summarises the magnitude of oxygen and carbon vital effects found in the present study, compared to previously documented fractionation factors.

4.2.1. The oxygen isotope system

Our data confirm that both *E. huxleyi* and *G. oceanica* can be assigned to the isotopic "heavy group" on the basis of their $\delta^{18}O_c$ values. Compared to previous studies, the results of our very dilute batch cultures report significantly different magnitudes of the vital effect (Table 4). Indeed, the $\delta^{18}O$ offset seen for *G. oceanica* in this study is +1.27 ‰ (± 0.01 ‰) from equilibrium whereas Dudley et al. (1986) and Ziveri et al. (2003) obtained values between +2.4 and +2.9 ‰, respectively. It remains difficult to explain the "heavy group" thermodynamically for oxygen isotopes assuming a calcification substrate of HCO_3^-, as suggested by the experiments of Nimer and Merrett (1993) and Sekino and Shiraiwa (1944). There have been several studies demonstrating a large CO_2 diffusive supply to *E. huxleyi* relative to its carbon requirement owing to its small size and high area-to-volume ratio of the cell (Dong et al., 1993; Nimer et al., 1997; Nimer and Merrett, 1996; Bach et al., 2013). CO_2 has the heaviest oxygen isotope composition of all DIC species and water (Usdowski et al., 1991). We speculate that the fast division rate of *E. huxleyi*, and the high and continuous production of coccoliths by this species (Westbroek et al., 1989; Balch et al., 1993) result in the mineralisation of the internal pool of DIC before complete equilibrium readjustment is achieved. Hence, the coccoliths record to some extent the isotopically heavy oxygen isotope inherited of the CO_2. As *G. oceanica* is bigger (i.e. has reduced CO_2 passive diffusion) and divides more slowly relative to *E. huxleyi*, coccoliths produced by this species are closer to equilibrium. Our ^{18}O addition experiments indeed confirm a longer residence time of the DIC before calcification in *G. oceanica* compared to *E. huxleyi*, and thus a higher degree of isotopic erasing of the original CO_2 signature in the former.

The relatively large and slow growing *C. braarudii* precipitates calcite with $\delta^{18}O_c$ composition close to that of equilibrium calcite, as found in previous studies (Rickaby et al., 2010; Stevenson et al., 2014). This finding is, however, in slight contradiction to the work of Ziveri et al. (2003). In this latter work, this taxon was assigned to the isotopic "heavy group"

with a magnitude in $^{18}O/^{16}O$ fractionation comparable to that of *G. oceanica* (Table 4). Hence, in the view of the direction and magnitude of the vital effect in the oxygen isotopes (Eq. 4), *C. braarudii* cannot be assigned to the light or heavy group. Instead, the near-equilibrium $^{18}O/^{16}O$ fractionation would suggest that this large species can be assigned to a tentative "equilibrium group", as confirmed by other studies (Rickaby et al., 2010; Stevenson et al., 2014). This species has a very low specific growth rate (on the order of one division every three days, for the experimental conditions of the present study). Hence, the oxygen isotopes of the $H_2O - CO_2 - HCO_3^- - CO_3^{2-}$ system should be in constant thermodynamic equilibrium due to a high residence time of the DIC within the cell, such that the heavy oxygen isotope signature of CO_2 is completely erased before calcification. For this species, changing pCO_2 / ambient DIC levels has a great influence on $\delta^{18}O_c$ with isotopic values becoming heavier under higher CO_2 availability in the culturing medium (Rickaby et al., 2010). With more CO_2, the rate of passive diffusion may alleviate carbon limitation, resulting in a fertilisation of growth rate with faster overturning of the internal DIC pool. Together, this results in a diminution of the residence time of DIC in the cytosol preventing complete re-equilibration of the CO_2 isotopic signature. This process is likely to explain heavier $\delta^{18}O_c$ with increased DIC concentrations in the growth medium, and may explain the discrepancy between this study and that of Ziveri et al. (2003).

The coccolithophore *C. leptoporus* produces calcite that is isotopically lighter than predicted for oxygen isotopic equilibrium with an offset by ~ –1 ‰. This offset may imply that the $\delta^{18}O$ of the pool of DIC that serves for calcite precipitation may be shifted towards the signature of the carbonate CO_3^{2-} ion ($\Delta\ \delta^{18}O_{\text{carbonate ion}} - \delta^{18}O_{\text{bicarbonate}} \sim -16$ ‰). *C. leptoporus* produces a relatively small amount of organic matter compared to *E. huxleyi* and *G*. oceanica. For *C. leptoporus*, this $\delta^{18}O$ shift can be achieved through raising *p*H and

increasing [CO_3^{2-}] inside the cell (Zeebe, 1999), corresponding the "carbonate ion effect" described by Ziveri et al. (2012).

4.2.2. The carbon isotope system

The carbon system in solution is restricted to the DIC molecules, and hence does not re-equilibrate with H_2O molecules. Therefore the $\delta^{13}C$ of the internal pool of DIC is primarily dictated by the nature of DIC assimilation, either by active or passive supply, without subsequent equilibriation, as occurs in the oxygen isotopic system. In this case, even if at *p*H ~ 7 in the cytosol (Anning et al., 1996), the CO_2 will be hydrated and converted into HCO_3^-, the composition of the whole DIC pool will still maintain a negative $\delta^{13}C$.

It may appear surprising that *E. huxleyi,* for which a dominant CO_2 acquisition is demonstrated at "normal" ambient CO_2 levels (Nimer et al., 1999) has substantially high $\delta^{13}C_c$. Indeed, the $\delta^{13}C$ of CO_2 is the lightest of all the DIC species (Mook, 1986; Zeebe and Wolf-Gladrow, 2001; Zhang et al., 2005). *E. huxleyi* and *G. oceanica* are the two species that produced the most organic matter with respect to calcite (lowest PIC/POC ratios; Table 1). Fixation of CO_2 by photosynthesis favours incorporation of ^{12}C (Freeman and Hayes, 1992; Laws et al., 2002). As a result, the intracellular carbon pool of these species is likely to be most affected by the large kinetic isotope fractionation accompanying CO_2 fixation by photosynthesis, up to ~ 30 ‰ (Laws et al., 2002). The remaining pool of DIC available for calcification becomes progressively ^{12}C-depleted. We hypothesise that the internal pool evolves according to Rayleigh distillation towards heavier values of $\delta^{13}C_{DIC}$, which is then reflected in the high $\delta^{13}C$ of the coccoliths. The influence of stable isotope fractionation in the organic matter on the isotopic composition of calcium carbonate is compatible with the idea that both carbon fixation pathways "share" a common pool of DIC (Rokitta and Rost, 2012). Considering PIC/POC ratios, growth rates, and cell sizes together (Eq. 1; Table 1), this

hypothesis is able to explain why *E. huxleyi* is more offset towards high $\delta^{13}C_c$ than *G. oceanica* with respect to equilibrium, a consistent finding in all culture datasets (Stoll and Ziveri, 2004). This point indicates that the +1 to +3 ‰ offset relative to equilibrium documented for *G. oceanica* and *E. huxleyi* does not reflect a physiological process related to calcification itself, as it seems to depend on the intensity of photosynthesis over calcification. This may explain why different degrees of fractionation leading to higher $\delta^{13}C_c$ but also $\delta^{18}O_c$ are documented in the literature compared to those found in this study (Table 4). This "reservoir effect" may correspond to a culture artefact and represent a caveat for proposing reliable fractionation factors for the isotopic "heavy group". In the study of Moolna and Rickaby (2012), this $\delta^{13}C$ drift affected the culture medium itself, so it is unclear whether this process affects the intracellular carbon pool or the whole system calling into question implementation of even dilute batch cultures for investigating carbon isotope fractionation in coccolith calcite. It is plausible that in unlimited DIC conditions, as in the open ocean, the Rayleigh distillation does not operate due to constant renewal of the DIC, and enhanced exchange between the internal and external pools of DIC.

The coccoliths of *C. braarudii* present relatively light $\delta^{13}C_c$ values that are compatible with a predominant acquisition of CO_2 by passive diffusion. Assuming the same CO_2 source, the discrepancy between *E. huxleyi* and *C. braarudii* illustrates the vital effect on stable isotope fractionation. The carbon isotopes in *C. braarudii* maintain the negative $\delta^{13}C_{DIC}$ characteristic of a CO_2 source (Zeebe and Wolf-Gladrow, 2001) with little effect from a Rayleigh distillation driven by photosynthetic fractionation, contrary to *E. huxleyi*. As described above for the oxygen isotopes, significant change in $\delta^{13}C_c$ of *C. braarudii* has ben reported with increased DIC concentrations in the culture medium (Rickaby et al., 2010). Not only does the increased CO_2 supply enhance growth rate, but it also increases photosynthetic carbon fixation leading to lower PIC/POC ratios (Gerecht et al., 2014). With more

partitioning of carbon into the organic matter, the carbon isotope composition of the coccoliths becomes driven by a Rayleigh fractionation system, as described for *E. huxleyi.*

The higher PIC/POC ratio of *C. leptoporus* compared to *C. braarudii* under "normal" CO_2 concentrations explains the more negative $\delta^{13}C_c$ composition of *C. leptoporus,* which is closer to the CO_2 source because this species is the less affected by RubisCO ^{12}C fractionation from all examined cells.

4.3. Stable isotope fractionation in the dinoflagellate *Thoracosphaera heimii*

Thoracosphaera heimii belongs, as the coccolithophore *Calcidiscus leptoporus*, to the isotopically light group for $\delta^{18}O$. At face value, *T. heimii* calcispheres may also record the oxygen isotopic composition of CO_3^{2-}. For both species, the concentration of carbonate ions has proven to be influential on the $\delta^{18}O$ of calcite, with an even stronger effect than *C. leptoporus* (Ziveri et al., 2012; Van de Waal et al., 2013). The magnitude in $^{13}C/^{12}C$ fractionation is in agreement with the extremely light carbon isotope compositions observed by Zonneveld et al. (2007). The negative $\delta^{13}C_c$ compared to coccoliths and inorganically precipitated calcite may also be compatible with the carbonate ion isotopic signature ($\Delta\ \delta^{13}C_{carbonate\ ion} - \delta^{13}C_{bicarbonate} \sim -2$ ‰) although the $^{13}C/^{12}C$ fractionation of –3.5 ‰ would suggest a contribution of an isotopically lighter source as CO_2 ($\Delta\ \delta^{13}C_{carbon\ dioxide} - \delta^{13}C_{bicarbonate} \sim -9$ ‰). It has been proposed that calcification in calcareous dinoflagellates partly occurs extracellularly (Inouye and Pienaar, 1983). Hence, precipitation of calcite by *T. heimii* is likely to occur in a less biologically controlled system than inside coccolith vesicles. Although *T. heimii* is characterised by relative high carbon fixation by photosynthesis with respect to calcification (same order of magnitude as *E. huxleyi*), it appears that the carbon isotope system is less coupled between photosynthesis and calcification with $\delta^{13}C_c$ remaining

negative, as imposed by a CO_2 substrate. This point represents supplementary evidence for a more open system in terms of the carbon pool in dinoflagellates than in coccolithophores. This biogeochemical feature indicates that light carbon isotope composition in dinoflagellate calcite has to be understood in terms of a pristine CO_2 isotopic signal, rather than possible remineralisation of respired carbon in this group (Friedrich and Meier, 2003).

4.4. Implication for SST reconstruction using $\delta^{18}O$ of biogenic carbonate

The reconstitution of seawater palaeotemperatures using oxygen isotope composition of carbonate shells (foraminifera and coccoliths) can be biased by two main factors: the global volume of ^{18}O-depleted ice (as this affects the isotopic composition of seawater), and the biological imprint on $^{18}O/^{16}O$ fractionation (vital effect). Most culture and core-top studies have addressed this latter point by investigating the sensitivity of oxygen isotopes in $CaCO_3$ to temperature for a near constant $\delta^{18}O_w$ (Erez and Luz, 1983; Dudley et al., 1986; Bemis et al., 1998; Ziveri et al., 2003; Candelier et al., 2013). Our experiments show that changing the $\delta^{18}O_w$ of the culturing medium also leads to variable alterations in the magnitude of the vital effect, ranging from no influence for *G. oceanica* to significant influence for *C. leptoporus* (~ 1.7 % per 10 ‰ change in $\delta^{18}O_w$). This result may call into question the use of the geochemical signature of coccoliths for palaeotemperature reconstructions. Using the equation determined by Candelier et al. (2013) for *C. leptoporus*, we calculated a calcification temperature of 14.9 °C using our $\delta^{18}O_c - \delta^{18}O_w$ for a $\delta^{18}O_w$ of +0.69 ‰ [V-SMOW]. For a $\delta^{18}O_w$ of ~ +6 ‰, the inferred temperature is 21 °C, which is a significant offset compared to the actual temperature of 15 °C. Thus, if we try and calculate SST using monospecific assemblages of *C. leptoporus* retrieved from a core top ($\delta^{18}O_w$ ~ 0 ‰) and from a samples

spanning the LGM ($\delta^{18}O_w$ ~ 1.1 ‰; Schrag et al., 2002), we can expect a bias of 1.15 °C (Fig. 5).

More generally, the non-equilibrium changes in $^{18}O/^{16}O$ fractionation with changing $\delta^{18}O_w$ may introduce bias for many other taxa of marine calcifiers, which will impact the derivation of robust SSTs from $\delta^{18}O_c$. Whilst we acknowledge that the range of δ^{18}Ow applied in our experiments are ten-fold those documented throughout the Meso-Cenozoic, this potential bias in SST reconstruction is best illustrated by *C. leptoporus* and *G. oceanica*, which have the most divergent responses (Fig. 5). The implication for this effect is that seawater temperatures, estimated using $\delta^{18}O$ of coccolith calcite, will contain a significant bias depending on the species under investigation. In contrast to the behaviour of *C. leptoporus*, the magnitude of $^{18}O/^{16}O$ fractionation in *Gephyrocapsa oceanica* is not sensitive to the absolute isotopic value of the water. As such, the temperature dependence equations of Ziveri et al. (2003) for *G. oceanica*, and by extension for the reticulofenestrids, can be applied to any time period.

Further, the discrepancy between different taxa provides information on absolute seawater $\delta^{18}O$ values. That is, the oxygen isotopic offset between coeval *G. oceanica* and *C. leptoporus* will be proportional to the $\delta^{18}O_w$ of the mineralising fluid. This discrepancy may therefore be useful in the geological record when trying to decouple the relative influences of temperature and ice volume in the oxygen isotopic composition of sedimentary $CaCO_3$.

5. CONCLUSIONS

Vital effects lead to physiologically mediated offsets in calcifying plankton that can drive precipitated biominerals away from predicted inorganic isotopic compositions. The results from our culture-based study of coccolithophores and calcareous dinoflagellates

demonstrate that the magnitude of the vital effect also depends on the oxygen isotopic composition of the mineralising fluid. By systematically investigating the magnitude of this offset under a range of seawater $\delta^{18}O$ across multiple taxa, we hypothesise that the carbon and oxygen isotope composition of biogenically precipitated calcite is controlled by the dynamics of the carbon pool (supply versus demand) and the partitioning of DIC between photosynthesis and calcification. Future studies that attempt to quantity the size of the internal DIC pools will help place quantitative constraints on the dynamics of the oxygen isotope system from acquisition to mineralisation of calcium carbonate. Overall, our data underscore the coupling between photosynthetic and mineralising pathways in the fixation of carbon in phytoplankters that affects both the carbon and oxygen isotopic systems. The likely explanation for high $\delta^{18}O_c$ values in *E. huxleyi* and *G. oceanica* ("heavy group") is a source effect inherited from the CO_2 signature in fast growing systems, and a reservoir effect due to progressive ^{12}C depletion of the intracellular DIC pool for high $\delta^{13}C_c$. Large coccolithophore cells, also characterised by higher calcification over photosynthesis rates and lower growth rates are, as a result, closer to equilibrium for the oxygen isotopes and to the composition of the source, presumably CO_2, for the carbon isotopes. Our data confirm a double contribution of an intra- and extra-cellular calcification for calcareous dinoflagellates. This study illustrates the potential of an interspecies proxy of the coccoliths to reconstruct palaeo-DIC concentrations and $\delta^{18}O$ of seawater.

Acknowledgments. We owe thanks to Nathalie Labourdette and Norman Charnley for assistance in the preparation of the $\delta^{18}O$-modified solutions, and running of the mass spectrometers. Coccolithophore strains were provided by the Roscoff Culture Collection to MH via the EU FP7 Research Infrastructure Initiative "ASSEMBLE" Ref. 227799. This work benefited from insightful discussions with Harry McClelland, Yaël Candelier, Chris Day,

Giovanni Aloisi and Gideon Henderson. We thank Clara Bolton, an anonymous reviewer and the Associate Editor Claire Rollion-Bard insightful comments on a previous version of the manuscript. MH is grateful to the Natural Environment Research Council (NERC) for funding through Postdoctoral Fellowship (NE/H015523/1). TJH is supported by the Postdoctoral Scholar Program at the Woods Hole Oceanographic Institution, with funding provided by the Doherty Foundation. REMR was supported through European Research Council (ERC) grant SP2-GA-2008-200915.

6. REFERENCE LIST

Anning T, Nimer N., Merrett M. J. and Brownlee C. (1996) Costs and benefits of calcification in coccolithophorids. *J. Mar. Syst.* **9**, 45–56.

Bach L. T., Mackinder L. C. M., Schulz K. G., Wheeler G., Schroeder D. C., Brownlee C. and Riebesell U. (2013) Dissecting the impact of CO_2 and pH on the mechanisms of photosynthesis and calcification in the coccolithophore Emiliania huxleyi. *New Phytol.* **199**, 121–34.

Balch W. M., Kilpatrick K., Holligan P. M. and Cucci T. (1993) Coccolith production and detachment by *Emiliania huxleyi* (Prymnesiophyceae). *J. Phycol.* **29**, 566–575.

Beck W. C., Grossman E. L. and Morse J. W. (2005) Experimental studies of oxygen isotope fractionation in the carbonic acid system at 15°, 25°, and 40°C. *Geochim. Cosmochim. Acta* **69**, 3493–3503.

Behar F., Beaumont V. and De B. Penteado H. L. (2001) Rock-Eval 6 Technology: Performances and Developments. *Oil Gas Sci. Technol.* **56**, 111–134.

Bemis B. E., Spero H. J., Bijma J. and Lea D. W. (1998) Reevaluation of the oxygen isotopic composition of planktonic foraminifera: Experimental results and revised

paleotemperature equations. *Paleoceanogr.* **13**, 150–160, doi:10.1029/98PA00070.

Bolton C. T. and Stoll H. M. (2013) Late Miocene threshold response of marine algae to carbon dioxide limitation. *Nature* **500**, 558–562.

Bolton C. T., Stoll H. M. and Mendez-Vicente A. (2012) Vital effects in coccolith calcite: Cenozoic climate - pCO_2 drove the diversity of carbon acquisition strategies in coccolithophores? *Paleoceanography* **27**, 1–16.

Brand W. A., Assonov S. S. and Coplen T. B. (2010) Correction for the ^{17}O interference in δ(13C) measurements when analyzing CO_2 with stable isotope mass spectrometry (IUPAC Technical Report). *Pure Appl. Chem.* **82**, 1719–1733.

Broecker W. and Clark E. (2009) Ratio of coccolith $CaCO_3$ to foraminifera $CaCO_3$ in late Holocene deep sea sediments. *Paleoceanography*, **24,** 1–11.

Candelier Y., Minoletti F., Probert I. and Hermoso M. (2013) Temperature Dependence of Oxygen Isotope Fractionation in Coccolith Calcite: A Culture and Core Top Calibration of the genus *Calcidiscus*. *Geochim. Cosmochim. Acta* **100**, 264–281.

Dong B. Y. L. F., Nimer N. A., Okus E. and Merrett M. J. (1993) Dissolved inorganic carbon utilization in relation to calcite production in *Emiliania huxleyi* (Lohmann) Kamptner. *New Phytol.* **123**, 679–684.

Dudley W. C., Blackwelder P., Brand L. and Duplessy J.-C. (1986) Stable isotopic composition of coccoliths. *Mar. Micropaleontol.* **10**, 1–8.

Erez J. and Luz B. (1983) Experimental paleotemperature equation for planktonic foraminifera. *Geochim. Cosmochim. Acta* **47**, 1025–1031.

Freeman K. H. and Hayes J. M. (1992) Fractionation of carbon isotopes by phytoplankton and estimates of ancient CO_2 levels. *Global Biogeochem. Cycles* **6**, 185–198.

Friedrich O. and Meier K. J. S. (2003) Stable isotopic indication for the cyst formation depth of Campanian/Maastrichtian calcareous dinoflagellates. *Micropaleontology* **49**, 375–

380.

Gerecht A. C., Šupraha L., Edvardsen B., Probert I. and Henderiks J. (2014) High temperature decreases the PIC / POC ratio and increases phosphorus requirements in *Coccolithus pelagicus* (Haptophyta). *Biogeosciences Discuss.* **11**, 1021–1051.

Giordano M., Beardall J. and Raven J. A. (2005) CO_2 concentrating mechanisms in algae: Mechanisms, environmental modulation, and evolution. *Annu. Rev. Plant Biol.* **56**, 99–131.

Guillard R. R. L. (1975) Culture of phytoplankton for feeding marine invertebrates. In *Culture of Marine Invertebrate Animals* (eds. W. L. Smith and M. H. Chanley). Plenum Press, New York, pp. 26–60.

Hermoso M., Le Callonnec L., Minoletti F., Renard M. and Hesselbo S. P. (2009) Expression of the Early Toarcian negative carbon-isotope excursion in separated carbonate microfractions (Jurassic, Paris Basin). *Earth Planet. Sci. Lett.* **277**, 194–203.

Hermoso M., Minoletti F., Candelier Y., McClelland H.L., Aloisi G. and Rickaby R.E.M. (2013) Calcification rate and carbon-isotope fractionation in coccolithophore calcite through laboratory culture experiments. *Min. Mag*. **77**, p. 1290.

Inouye I. and Pienaar R. N. (1983) Observations on the life-cycle and microanatomy of *Thoracosphaera heimii* (dinophyceae) with special reference to its systematic position. *S. Afr. J. Bot.* **2**, 63-75.

Keller M. D., Selvin R. C., Claus W. and Guillard R. R. L. (1987) Media for the culture of oceanic ultraphytoplankton. *J. Phycol.* **23**, 633–638.

Kim S. T. and O'Neil J. R. (1997) Equilibrium and non equilibrium oxygen isotope effects in synthetic carbonates. *Geochim. Cosmochim. Acta* **61**, 3461–3475.

Langer G., Geisen M., Baumann K.-H., Kläs J., Riebesell U., Thoms S. and Young J. R. (2006) Species-specific responses of calcifying algae to changing seawater carbonate

chemistry. *Geochemistry Geophys. Geosystems* **7**, Q09006, doi:10.1029/2005GC001227.

Langer G., Nehrke G., Probert I., Ly J. and Ziveri P. (2009) Strain-specific responses of *Emiliania huxleyi* to changing seawater carbonate chemistry. *Biogeosciences* **6**, 2637–2646.

Laws E. A., Popp B. N., Cassar N. and Tanimoto J. (2002) ^{13}C discrimination patterns in oceanic phytoplankton: likely influence of CO_2 concentrating mechanisms, and implications for palaeoreconstructions. *Funct. plant Biol.* **29**, 323–333.

Minoletti F., Hermoso M. and Gressier V. (2009) Separation of sedimentary micron-sized particles for palaeoceanography and calcareous nannoplankton biogeochemistry. *Nat. Protoc.* **4**, 14–24.

Mook W. G. (1986) ^{13}C in atmospheric CO_2. *Netherlands J. Sea Res.* **20**, 211–223.

Moolna A. and Rickaby R. E. M. (2012) Interaction of the coccolithophore *Gephyrocapsa oceanica* with its carbon environment: response to a recreated high-CO_2 geological past. *Geobiology* **10**, 72–81.

Nimer N. A. and Merrett M. J. (1993) Calcification rate in *Emiliania huxleyi* Lohmann in response to light, nitrate and availability of inorganic carbon. *New Phytol.* **123**, 673–677.

Nimer N., Guan Q. and Merrett M. J. (1994) Extra- and intracellular carbonic anhydrase in relation to culture age in a high calcifying strain of *Emiliania huxleyi* Lohman. *New Phytol.* **126**, 601–607.

Nimer N. A. and Merrett M. J. (1996) The development of a CO_2-Concentrating Mechanism in *Emiliania huxleyi*. *New Phytol.* **133**, 383–389.

Nimer N. A., Iglesias-Rodriguez M. D. and Michaelj M. (1997) Bicarbonate utilization by marine phytoplankton species. *J. Phycol.* **631**, 625–631.

Nimer N. A., Ling M. X., Brownlee C. and Merrett M. J. (1999) Inorganic carbon limitation, exofacial carbonic anhydrase activity, and plasma membrane redox activity in marine phytoplankton species. *J. Phycol.* **1205**, 1200–1205.

Rickaby R. E. M., Henderiks J. and Young J. (2010) Perturbing phytoplankton: response and isotopic fractionation with changing carbonate chemistry in two coccolithophore species. *Clim. Past* **6**, 771–785.

Robbins L.L., Hansen M.E., Kleypas J.A. and Meylan S.C. (2010) CO2calc—A user-friendly seawater carbon calculator for Windows, Max OS X, and iOS (iPhone). *U.S. Geological Survey Open-File Report* **2010–1280**, 17 p.

Rokitta SD and Rost B (2012) Effects of CO_2 and their modulation by light in the life-cycle stages of the coccolithophore *Emiliania huxleyi*. *Limnol. Oceanogr.* **57**, 607–618.

Rollion-Bard C., Chaussidon M. and France-Lanord C. (2011) Biological control of internal pH in scleractinian corals: Implications on paleo-pH and paleo-temperature reconstructions. *Comptes Rendus Geosci.* **343**, 397–405.

Romanek C. S., Grossman E. L. and Morse J. W. (1992) Carbon isotopic fractionation in synthetic aragonite and calcite: Effects of temperature and precipitation rate. *Geochim. Cosmochim. Acta* **56**, 419–430.

Santrock J., Studley S. A and Hayes J. M. (1985) Isotopic analyses based on the mass spectrum of carbon dioxide. *Anal. Chem.* **57**, 1444–1448.

Schrag D. P., Adkins J. F., McIntyre K., Alexander J. L., Hodell D. A., Charles C. D. and McManus J. F. (2002) The oxygen isotopic composition of seawater during the Last Glacial Maximum. *Quat. Sci. Rev.* **21**, 331–342.

Sekino K. and Shiraiwa Y. (1994) Accumulation and utilization of dissolved inorganic carbon by a marine unicellular coccolithophorid, *Emiliania huxleyi*. *Plant. Cell Physiol.* **35**, 353–361.

Stevenson E.I., Hermoso M., Rickaby R.E.M., Tyler J.J., Minoletti F., Parkinson I.J., Mokadem F. and Burton K.W. (2014) Controls on Stable strontium isotope fractionation in coccolithophores with implications for the marine Sr cycle. *Geochim. Cosmochim. Acta* **128**, 225–235.

Stoll H. M. (2005) Limited range of interspecific vital effects in coccolith stable isotopic records during the Paleocene-Eocene thermal maximum. *Paleoceanography* **20**, PA001016, doi.wiley.com/10.1029/2004PA001046.

Stoll H. and Ziveri P. (2004) Coccolithophore-based geochemical proxies. In *Coccolithophores: From Molecular Processes to Global Impact* (eds. H. R. Thierstein and J. Young). Springer, Berlin. pp. 529–562.

Tangen K., Brand L. E., Blackwelder P. L. and Guillard R. R. L. (1982) *Thoracosphaera heimii* (Lohmann) Kamptner is a dinophyte: Observations on its morphology and life cycle. *Mar. Micropaleontol.* **7**, 193–212.

Usdowski E., Michaelis J., Böttcher M. E. and Hoefs J. (1991) Factors for the oxygen isotope equilibrium fractionation between aqueous and gaseous CO_2, carbonic acid, bicarbonate, carbonate, and water (19°C). *Z. Phys. Chem.* **170**, 237–249.

Van de Waal D. B., John U., Ziveri P., Reichart G.-J., Hoins M., Sluijs A. and Rost B. (2013) Ocean acidification reduces growth and calcification in a marine dinoflagellate. *PLoS One* **8**, e65987.

Watkins J. M., Nielsen L. C., Ryerson F. J. and DePaolo D. J. (2013) The influence of kinetics on the oxygen isotope composition of calcium carbonate. *Earth Planet. Sci. Lett.* **375**, 349–360.

Weiner S. and Dove P.M (2003) An Overview of Biomineralization Processes and the Problem of the Vital Effect. *Rev. Mineral. Geochemistry* **54**, 1–29.

Westbroek P., Young J. R. and Linschooten K. (1989) Coccolith Production

(Biomineralization) in the Marine Alga *Emiliania huxleyi*. *J. Protozool.* **36**, 368–373.

Zachos J. C., Pagani M., Sloan L., Thomas E. and Billups K. (2001) Trends, rhythms, and aberrations in global climate 65 Ma to present. *Science* **292**, 686–693.

Zeebe R. (1999) An explanation of the effect of seawater carbonate concentration on foraminiferal oxygen isotopes. *Geochim. Cosmochim. Acta* **63**, 2001–2007.

Zeebe R. E. (2009) Hydration in solution is critical for stable oxygen isotope fractionation between carbonate ion and water. *Geochim. Cosmochim. Acta* **73**, 5283–5291.

Zeebe R. E. and Wolf-Gladrow D. (2001) *CO_2 in seawater: equilibrium, kinetics, isotopes*. Elsevier, Amsterdam.

Zhang J., Quay P. D. and Wilbur D. O. (1995) Carbon isotope fractionation during gas-water exchange and dissolution of CO_2. *Geochim. Cosmochim. Acta* **59**, 107–114.

Ziveri P., Stoll H., Probert I., Klaas C., Geisen M., Ganssen G. and Young J. (2003) Stable isotope vital effects in coccolith calcite. *Earth Planet. Sci. Lett.* **210**, 137–149.

Ziveri P., Thoms S., Probert I., Geisen M. and Langer G. (2012) A universal carbonate ion effect on stable oxygen isotope ratios in unicellular planktonic calcifying organisms. *Biogeosciences* **9**, 1025–1032.

Zonneveld K. A. F., Mackensen A. and Baumann K.-H. (2007) Stable oxygen isotopes of *Thoracosphaera heimii* (Dinophyceae) in relationship to temperature; a culture experiment. *Mar. Micropaleontol.* **64**, 80–90.

TABLE AND FIGURE CAPTIONS

Figure 1: Change in the oxygen (a) and carbon (b) isotope composition of precipitated calcite and DIC in solution with increasing $\delta^{18}O_w$ of the medium. For the oxygen isotope, the slope is slightly inferior to 1, an effect of the co-addition of ^{17}O atoms with the spiking of ^{18}O. This is

an artefact due to the mass spectrometric determination of $\delta^{18}O$ in which the abundance of ^{17}O is taken into account, thus "interfering" with the calculation of the $^{18}O/^{16}O$ ratio ("^{17}O artefact"; Santrock et al., 1985). For the carbon isotopes, the effect of ^{17}O co-addition is greater and results in a decrease in $\delta^{13}C$ (–0.03 ‰ in $\delta^{13}C$ per ‰ of $\delta^{18}O_w$ increase). It has to be noted that this change in $^{13}C/^{12}C$ fractionation is only apparent, as the $^{12}C/^{13}C$ in solution and in carbonate do not vary with $\delta^{18}O_w$. The offset between $\delta^{13}C_{DIC}$ and $\delta^{13}C_c$ is ~ 1 ‰, which is in agreement with the $\alpha_{calcite - bicarbonate}$ coefficient determined in the work by Romanek et al. (1992) (Eq. 3). Errors on the slopes are expressed as one standard deviation.

Figure 2: Raw oxygen (a) and carbon (b) isotope signature of coccolith and dinoflagellate calcite grown at 15 °C under a range of $\delta^{18}O_w$ from 0 to 75 ‰ (V-SMOW). In panel A, the blue dashed line represents the 1.00:0.98 line presented in Fig. 1a. In panel b, the inorganic calcite $\delta^{13}C$ is shown with an offset correction of 3.2 ‰ accounting for different initial $\delta^{13}C_{DIC}$ in both experimental set-up (inorganic versus cultures; Table 2). Errors on the slopes are expressed as one standard deviation. With the exception of *G. oceanica*, all species exhibit differential apparent $^{18}O/^{16}O$ fractionation with increased $\delta^{18}O_w$. Changes in apparent $^{13}C/^{12}C$ fractionation are explained by ^{17}O enrichment with increased $\delta^{18}O_w$, as seen in organic calcite. This effect is of same amplitude in solution, inorganic and biogenic calcite.

Figure 3: Changes in oxygen (a) and carbon (b) isotopic fractionation factors for the range of investigated $\delta^{18}O_w$. Lines represent the least squares fit for the culture and inorganic data (Fig. 2). The blue dashed lines represent the composition of precipitated calcite. For unmodified $\delta^{18}O$ medium (i.e. $\delta^{18}O_w$ close to 0 ‰), the taxa fall into three distinct isotopic groups: "heavy" (*E. huxleyi* and *G. oceanica*), "equilibrium" (*C. braarudii*), and "light" (*T. heimii* and *C. leptoporus)*. The effect of increasing $\delta^{18}O_w$ causes a reduction in $^{18}O/^{16}O$ apparent

fractionation, which is most pronounced for *C. leptoporus*. Low PIC/POC ratio species with maximum growth rates (*E. huxleyi* and *G. oceanica*) show "heavy" $^{13}C/^{12}C$ compositions, a possible reservoir effect caused by progressive depletion in ^{12}C by photosynthesis in the cellular pool of DIC and/or in the culturing medium. Other species show large fractionation towards light carbon isotopes, especially *T. heimii* (the isotopic record of CO_2 substrate).

Figure 4: Cross plot showing the relationship between oxygen isotope fractionation measured in unmodified $\delta^{18}O$ media and changes in apparent oxygen fractionation with ^{18}O addition in the culturing medium. Gradients correspond to the slopes of the linear regression shown in Fig. 3a. Errors bars in red are calculated from one standard deviation (1σ) of the linear regressions. There is a clear correlation between the effect on increasing ^{18}O abundance and reducing the apparent fractionation, with *Emiliania huxleyi* being an outlier, probably due to his very small PIC/POC ratio (see text). This link illustrates that the effect of reduction in the fractionation is more pronounced for species having an initial large offset towards negative $\delta^{18}O_c$ values.

Figure 5: Effect of the $\delta^{18}O_w$ of the medium on temperature estimates for *Calcidiscus leptoporus* (red filed circles) and *Gephyrocapsa oceanica* (blue open circles). Inference of seawater temperature is obtained via the calibration equations for these two taxa (Candelier et al., 2013; Ziveri et al., 2003). Regression lines are those established for the 0 – 75 ‰ interval. SST estimates are not affected for *G. oceanica* on the 5 ‰ change in $\delta^{18}O_w$ presented here as isotope temperatures match the actual growth temperature of 15 °C. By contrast, a bias or "$\delta^{18}O_w$ effect" is evident for *C. leptoporus.* Increasing $\delta^{18}O_w$ leads to increased temperature estimates. Using the example of the present-day and LGM oceans ($\delta^{18}O_w$ = 1.1 ‰ lighter than

today), the temperature for *C. leptoporus* calcite grown at 15 °C in an isotopically heavier seawater would be over-estimated at about 16.2 °C.

Table 1: Main characteristics of the coccolithophore and calcareous dinoflagellate taxa cultured in the present work. All the culture parameters are those corresponding to the experimental setup (K/2 medium; 15 °C; 250 μmol photons/m^2/s with a 14/10 light/dark cycle) and measured at beginning of the exponential growth phase (DIC replete conditions; ambient [DIC] ~ 2.3 mM). Further information for each strain can be obtained at http://www.sb-roscoff.fr/Phyto/RCC/. The PIC/POC ratio is a measurement of the partitioning of the DIC between the inorganic (calcification) and organic (photosynthesis) carbon fixation.

Table 2: Isotopic results for inorganically precipitated calcite.

Table 3: Isotopic results for cultures.

Table 4: Synthesis of vital effects ($\delta_c - \delta_{eq}$ in PDB) from literature data and new coefficients from the present study. "Corrected" previously reported vital effects are expressed with an inorganic reference using Eq. 2 (Kim and O'Neil, 1997 corrected for a *p*H 8.2) to allow comparison. For the carbon isotope system, the magnitude of fractionation is expressed relative to $\delta^{13}C_{bicarbonate}$ (~ $\delta^{13}C_{DIC}$).

Fig. 1

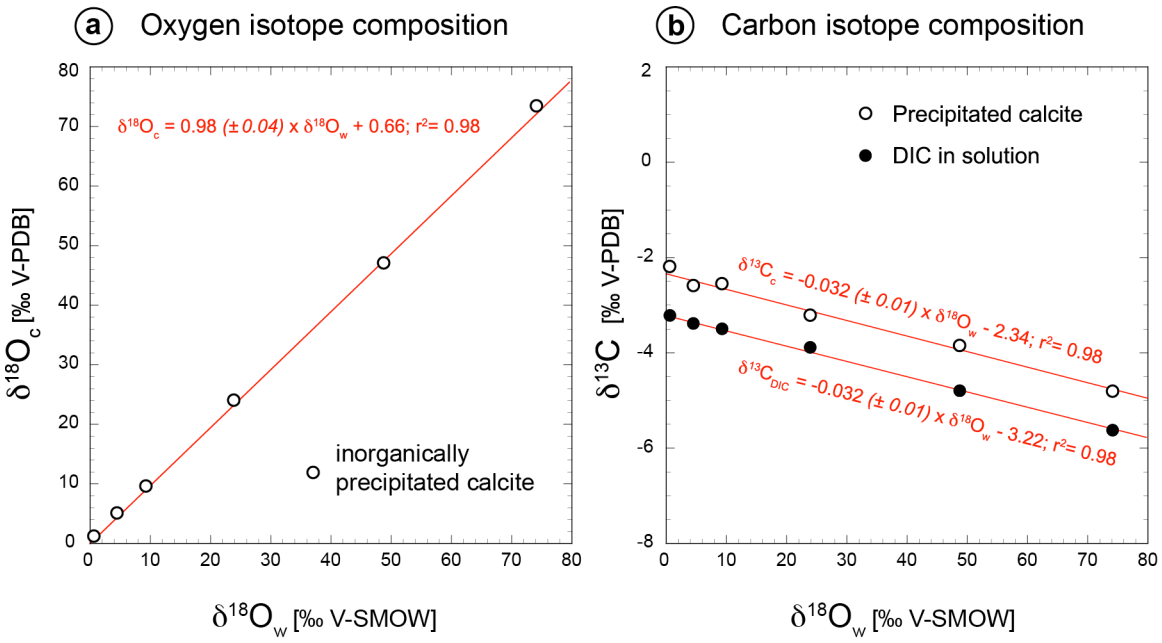
a Oxygen isotope composition
b Carbon isotope composition
δ18Oc = 0.98 (± 0.04) x δ18Ow + 0.66; r2= 0.98
inorganically precipitated calcite
δ18Oc [‰ V-PDB]
δ18Ow [‰ V-SMOW]
Precipitated calcite
DIC in solution
δ13Cc = -0.032 (± 0.01) x δ18Ow - 2.34; r2= 0.98
δ13CDIC = -0.032 (± 0.01) x δ18Ow - 3.22; r2= 0.98
δ13C [‰ V-PDB]
δ18Ow [‰ V-SMOW]

Fig. 2

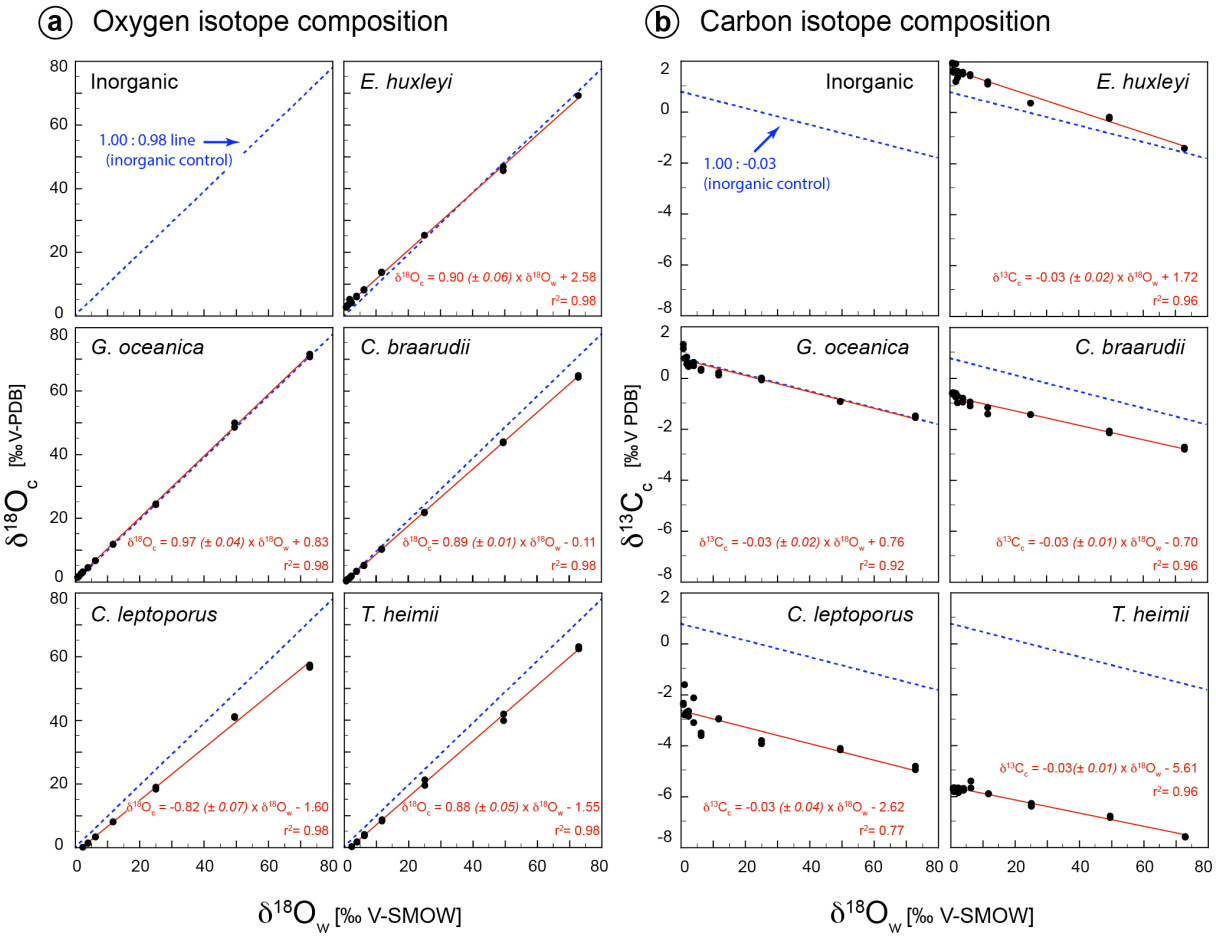
ⓐ Oxygen isotope composition
ⓑ Carbon isotope composition
Inorganic
1.00 : 0.98 line
(inorganic control)
E. huxleyi
δ18Oc = 0.90 (± 0.06) x δ18Ow + 2.58
r2= 0.98
G. oceanica
δ18Oc = 0.97 (± 0.04) x δ18Ow + 0.83
r2= 0.98
C. braarudii
δ18Oc = 0.89 (± 0.01) x δ18Ow - 0.11
r2= 0.98
C. leptoporus
δ18Oc = -0.82 (± 0.07) x δ18Ow - 1.60
r2= 0.98
T. heimii
δ18Oc = 0.88 (± 0.05) x δ18Ow - 1.55
r2= 0.98
δ18Oc [‰ V-PDB]
δ18Ow [‰ V-SMOW]
1.00 : -0.03
(inorganic control)
δ13Cc = -0.03 (± 0.02) x δ18Ow + 1.72
r2= 0.96
δ13Cc = -0.03 (± 0.02) x δ18Ow + 0.76
r2= 0.92
δ13Cc = -0.03 (± 0.01) x δ18Ow - 0.70
r2= 0.96
δ13Cc = -0.03 (± 0.04) x δ18Ow - 2.62
r2= 0.77
δ13Cc = -0.03(± 0.01) x δ18Ow - 5.61
r2= 0.96
δ13Cc [‰ V PDB]
δ18Ow [‰ V-SMOW]

Fig. 3

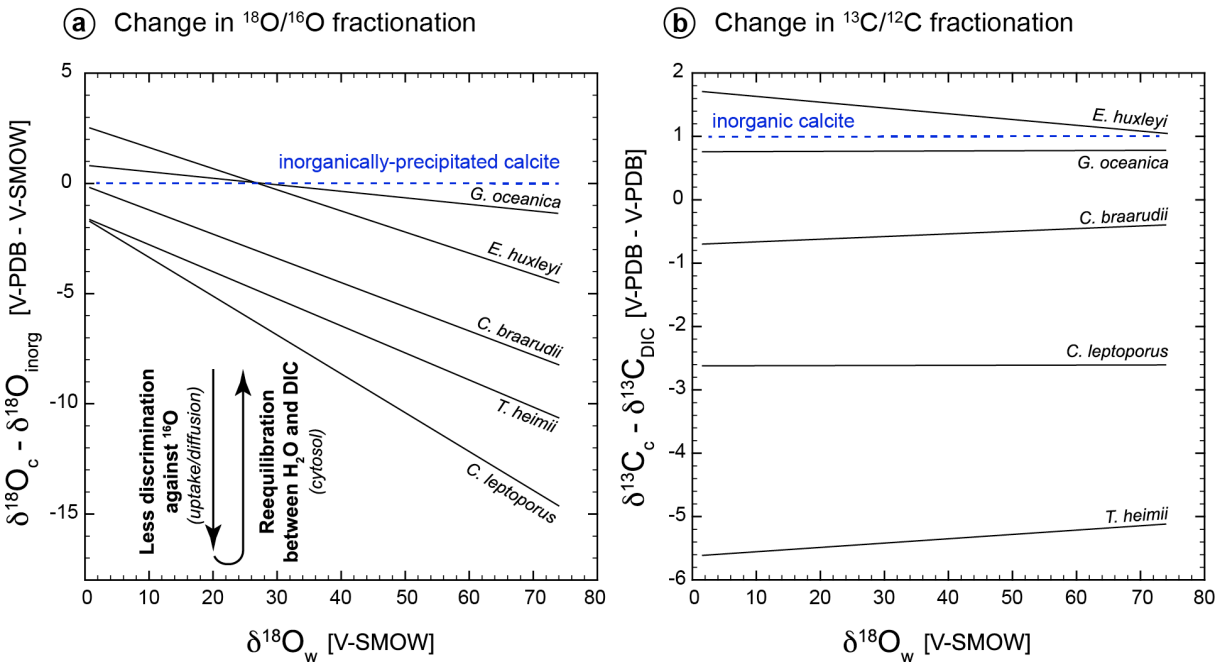
a Change in $^{18}O/^{16}O$ fractionation
b Change in $^{13}C/^{12}C$ fractionation
$\delta^{18}O_c - \delta^{18}O_{inorg}$ [V-PDB - V-SMOW]
$\delta^{18}O_w$ [V-SMOW]
inorganically-precipitated calcite
G. oceanica
E. huxleyi
C. braarudii
T. heimii
C. leptoporus
Less discrimination against ^{16}O (uptake/diffusion)
Reequilibration between H_2O and DIC (cytosol)
$\delta^{13}C_c - \delta^{13}C_{DIC}$ [V-PDB - V-PDB]
inorganic calcite

Fig. 4

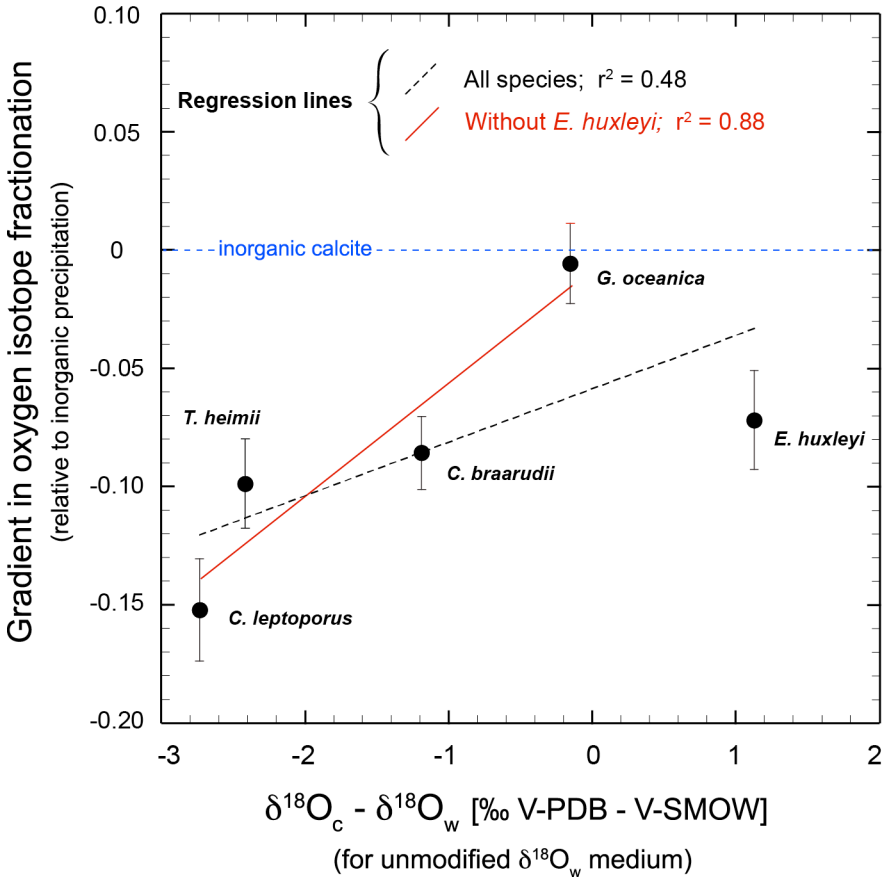
Regression lines
All species; r² = 0.48
Without E. huxleyi; r² = 0.88
inorganic calcite
G. oceanica
T. heimii
C. braarudii
E. huxleyi
C. leptoporus
Gradient in oxygen isotope fractionation
(relative to inorganic precipitation)
0.10
0.05
0
-0.05
-0.10
-0.15
-0.20
-3
-2
-1
0
1
2
δ18Oc - δ18Ow [‰ V-PDB - V-SMOW]
(for unmodified δ18Ow medium)

Fig. 5

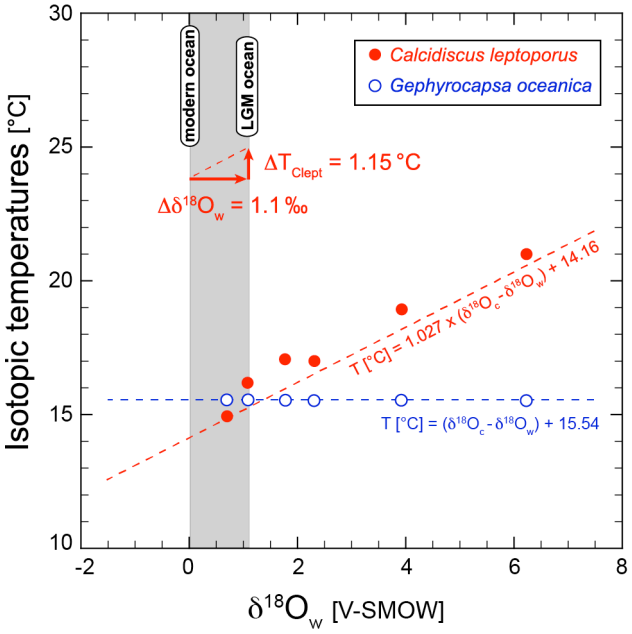
Isotopic temperatures [°C]
30
25
20
15
10
-2
0
2
4
6
8
δ18Ow [V-SMOW]
modern ocean
LGM ocean
Calcidiscus leptoporus
Gephyrocapsa oceanica
ΔTClept = 1.15 °C
Δδ18Ow = 1.1 ‰
T [°C] = 1.027 x (δ18Oc - δ18Ow) + 14.16
T [°C] = (δ18Oc - δ18Ow) + 15.54

Table 1

Species Name	**Roscoff Culture Collection ID**	**Region of Origin**	**Growth rate (μ)** [day^{-1}]	**Coccosphere size** [μm]	**Typical PIC/POC**
Gephyrocapsa oceanica	RCC 1314	Bay of Biscay	0.63	10	0.8
Emiliania huxleyi	RCC 1256	Islandic Coast	0.76	5	0.5
Coccolithus braarudii	RCC 1202	Portuguese Coast	0.32	20	2.9
Thoracosphaera heimii	RCC 1511	Japanese Coast	0.26	18	2
Calcidiscus leptoporus	RCC 1129	South Africa W Coast	0.38	17	3.1

Table 2

	$\delta^{18}O_w$ target	$\delta^{18}O_w$ measured	$\delta^{13}C_{DIC}$	$\delta^{13}C_c$	$\delta^{18}O_c$	Temp.	$\delta^{18}O_c$ - $\delta^{18}O_w$	$\delta^{18}O_{eq}$	$\delta^{13}C_c$ - $\delta^{13}C_{DIC}$	$\delta^{13}C_{eq}$
Inorganically precipitated calcite	1	0,56	-3,38	-2,18	1,29	15,00	0,73	0,13	1,20	-2,38
	5	4,45	-3,38	-2,58	5,18	15,00	0,74	4,02	0,80	-2,38
	10	9,23	-3,49	-2,54	9,72	15,00	0,48	8,81	0,95	-2,49
	25	23,88	-3,88	-3,21	24,12	15,00	0,25	23,45	0,67	-2,88
	50	48,69	-4,79	-3,84	47,19	15,00	-1,51	48,27	0,95	-3,79
	75	74,09	-5,62	-4,80	73,55	15,00	-0,54	73,66	0,82	-4,62

Table 3

Species	Replicate	$\delta^{18}O_w$ target	$\delta^{18}O_w$ measured	$\delta^{13}C_{DIC}$	$\delta^{13}C_c$	$\delta^{18}O_c$	Temp.	$\delta^{18}O_c - \delta^{18}O_w$	$\delta^{18}O_{eq}$	$\delta^{18}O_{inorg}$	VE ^{18}O	^{18}O offset from inorg	$\delta^{13}C_c - \delta^{13}C_{DIC}$	$\delta^{13}C_{eq}$	$\delta^{13}C_{inorg}$	VE ^{13}C	^{13}C offset from inorg
Gephyrocapsa oceanica	A	unmodified	0,69	-0,02	1,34	1,55	15,00	0,86	0,26	1,33	1,28	0,21	1,36	0,98	0,98	0,36	0,36
	B	unmodified	0,69	-0,02	1,18	1,53	15,00	0,84	0,26	1,33	1,26	0,19	1,20	0,98	0,98	0,20	0,20
	A	1	1,07	-0,03	0,78	1,95	15,00	0,88	0,64	1,70	1,31	0,25	0,81	0,97	0,97	-0,19	-0,18
	B	1	1,07	-0,03	0,79	1,89	15,00	0,82	0,64	1,70	1,25	0,19	0,82	0,97	0,97	-0,18	-0,17
	A	2	1,77	-0,06	0,56	2,76	15,00	0,99	1,34	2,39	1,41	0,37	0,62	0,94	0,94	-0,38	-0,38
	B	2	1,77	-0,06	0,85	2,66	15,00	0,89	1,34	2,39	1,32	0,27	0,91	0,94	0,94	-0,09	-0,10
	A	3	2,3	-0,07	0,59	3,17	15,00	0,87	1,87	2,91	1,29	0,26	0,66	0,93	0,93	-0,34	-0,33
	B	3	2,3	-0,07	0,47	3,31	15,00	1,01	1,87	2,91	1,43	0,40	0,54	0,93	0,93	-0,46	-0,46
	A	5	3,91	-0,13	0,50	4,66	15,00	0,75	3,48	4,48	1,17	0,18	0,63	0,87	0,87	-0,37	-0,38
	B	5	3,91	-0,13	0,64	4,52	15,00	0,61	3,48	4,48	1,04	0,04	0,77	0,87	0,87	-0,23	-0,23
	A	7	6,22	-0,20	0,37	6,83	15,00	0,61	5,79	6,73	1,04	0,10	0,57	0,80	0,80	-0,43	-0,43
	B	7	6,22	-0,20	0,32	6,78	15,00	0,56	5,79	6,73	0,98	0,05	0,52	0,80	0,80	-0,48	-0,48
	A	10	11,68	-0,38	0,23	11,90	15,00	0,22	11,25	12,06	0,65	-0,16	0,61	0,62	0,63	-0,39	-0,39
	B	10	11,68	-0,38	0,13	11,99	15,00	0,31	11,25	12,06	0,73	-0,07	0,51	0,62	0,63	-0,49	-0,49
	A	25	24,97	-0,81	0,02	24,38	15,00	-0,59	24,54	25,03	-0,17	-0,65	0,83	0,19	0,20	-0,17	-0,18
	B	25	24,97	-0,81	-0,06	24,65	15,00	-0,32	24,54	25,03	0,10	-0,38	0,75	0,19	0,20	-0,25	-0,26
	A	50	49,44	-1,61	-0,90	50,08	15,00	0,64	49,01	48,91	1,07	1,17	0,71	-0,61	-0,58	-0,29	-0,31
	B	50	49,44	-1,61	-0,91	48,72	15,00	-0,72	49,01	48,91	-0,29	-0,19	0,70	-0,61	-0,58	-0,30	-0,32
	A	75	72,78	-2,37	-1,53	71,68	15,00	-1,10	72,35	71,69	-0,67	0,00	0,84	-1,37	-1,33	-0,16	-0,20
	B	75	72,78	-2,37	-1,47	70,84	15,00	-1,94	72,35	71,69	-1,51	-0,85	0,90	-1,37	-1,33	-0,10	-0,13
Emiliania huxleyi	A	unmodified	0,69	-0,02	1,94	2,76	15,00	2,07	0,26	1,33	2,50	1,43	1,96	0,98	-2,36	0,96	4,31
	B	unmodified	0,69	-0,02	1,96	2,88	15,00	2,19	0,26	1,33	2,61	1,54	1,98	0,98	-2,36	0,98	4,33
	A	1	1,07	-0,03	1,59	3,30	15,00	2,23	0,64	1,70	2,66	1,60	1,62	0,97	-2,38	0,62	3,97
	B	1	1,07	-0,03	1,68	3,36	15,00	2,29	0,64	1,70	2,72	1,65	1,71	0,97	-2,38	0,71	4,06
	A	2	1,77	-0,06	1,23	4,11	15,00	2,34	1,34	2,39	2,77	1,72	1,29	0,94	-2,40	0,29	3,63
	B	2	1,77	-0,06	1,93	5,31	15,00	3,54	1,34	2,39	3,97	2,93	1,99	0,94	-2,40	0,99	4,33
	A	3	2,3	-0,07	1,38	4,17	15,00	1,87	1,87	2,91	2,30	1,26	1,45	0,93	-2,42	0,45	3,79
	B	3	2,3	-0,07	1,64	4,33	15,00	2,03	1,87	2,91	2,46	1,43	1,71	0,93	-2,42	0,71	4,06
	A	5	3,91	-0,13	1,53	6,03	15,00	2,12	3,48	4,48	2,55	1,56	1,66	0,87	-2,47	0,66	4,00
	B	5	3,91	-0,13	1,60	6,33	15,00	2,42	3,48	4,48	2,85	1,85	1,73	0,87	-2,47	0,73	4,07
	A	7	6,22	-0,20	1,51	8,17	15,00	1,95	5,79	6,73	2,38	1,44	1,71	0,80	-2,55	0,71	4,06
	B	7	6,22	-0,20	1,46	8,40	15,00	2,18	5,79	6,73	2,60	1,67	1,66	0,80	-2,55	0,66	4,00
	A	10	11,68	-0,38	1,22	13,68	15,00	2,00	11,25	12,06	2,42	1,62	1,60	0,62	-2,72	0,60	3,95
	B	10	11,68	-0,38	1,13	13,88	15,00	2,20	11,25	12,06	2,63	1,82	1,51	0,62	-2,72	0,51	3,85
	A	25	24,97	-0,81			15,00		24,54	25,03				0,19	-3,16		
	B	25	24,97	-0,81	0,39	25,45	15,00	0,48	24,54	25,03	0,90	0,42	1,20	0,19	-3,16	0,20	3,54
	A	50	49,44	-1,61	-0,22	46,98	15,00	-2,46	49,01	48,91	-2,03	-1,93	1,39	-0,61	-3,95	0,39	3,74
	B	50	49,44	-1,61	-0,17	45,76	15,00	-3,68	49,01	48,91	-3,25	-3,15	1,44	-0,61	-3,95	0,44	3,79
	A	75	72,78	-2,37	-1,39	69,30	15,00	-3,48	72,35	71,69	-3,05	-2,39	0,98	-1,37	-4,72	-0,02	3,32
	B	75	72,78	-2,37			15,00		72,35	71,69				-1,37	-4,72		
Coccolithus braarudii	A	unmodified	0,69	-0,02	-0,56	0,38	15,00	-0,31	0,26	1,33	0,12	-0,95	-0,54	0,98	-2,36	-1,54	1,80
	B	unmodified	0,69	-0,02	-0,60	0,62	15,00	-0,07	0,26	1,33	0,36	-0,71	-0,58	0,98	-2,36	-1,58	1,76
	A	1	1,07	-0,03	-0,60	0,92	15,00	-0,15	0,64	1,70	0,28	-0,78	-0,57	0,97	-2,38	-1,57	1,78
	B	1	1,07	-0,03	-0,56	0,96	15,00	-0,11	0,64	1,70	0,32	-0,75	-0,53	0,97	-2,38	-1,53	1,82
	A	2	1,77	-0,06	-0,58	1,32	15,00	-0,45	1,34	2,39	-0,02	-1,07	-0,52	0,94	-2,40	-1,52	1,82
	B	2	1,77	-0,06	-0,73	1,45	15,00	-0,32	1,34	2,39	0,11	-0,94	-0,67	0,94	-2,40	-1,67	1,67
	A	3	2,3	-0,07	-0,68	1,88	15,00	-0,42	1,87	2,91	0,01	-1,02	-0,61	0,93	-2,42	-1,61	1,73
	B	3	2,3	-0,07	-0,95	2,01	15,00	-0,29	1,87	2,91	0,13	-0,90	-0,88	0,93	-2,42	-1,88	1,47
	A	5	3,91	-0,13	-0,76	3,39	15,00	-0,52	3,48	4,48	-0,09	-1,09	-0,63	0,87	-2,47	-1,63	1,71
	B	5	3,91	-0,13	-0,93	3,52	15,00	-0,39	3,48	4,48	0,04	-0,96	-0,80	0,87	-2,47	-1,80	1,54
	A	7	6,22	-0,20	-0,92	5,38	15,00	-0,84	5,79	6,73	-0,42	-1,35	-0,72	0,80	-2,55	-1,72	1,63
	B	7	6,22	-0,20	-1,08	5,21	15,00	-1,01	5,79	6,73	-0,58	-1,52	-0,88	0,80	-2,55	-1,88	1,47
	A	10	11,68	-0,38	-1,39	10,48	15,00	-1,20	11,25	12,06	-0,78	-1,58	-1,01	0,62	-2,72	-2,01	1,33
	B	10	11,68	-0,38	-1,14	10,31	15,00	-1,37	11,25	12,06	-0,94	-1,75	-0,76	0,62	-2,72	-1,76	1,59
	A	25	24,97	-0,81	-1,41	21,84	15,00	-3,13	24,54	25,03	-2,70	-3,18	-0,60	0,19	-3,16	-1,60	1,74
	B	25	24,97	-0,81	-1,42	22,01	15,00	-2,97	24,54	25,03	-2,54	-3,02	-0,61	0,19	-3,16	-1,61	1,74
	A	50	49,44	-1,61	-2,06	44,14	15,00	-5,30	49,01	48,91	-4,88	-4,77	-0,45	-0,61	-3,95	-1,45	1,90
	B	50	49,44	-1,61	-2,13	43,80	15,00	-5,64	49,01	48,91	-5,22	-5,11	-0,52	-0,61	-3,95	-1,52	1,82
	A	75	72,78	-2,37	-2,69	64,96	15,00	-7,82	72,35	71,69	-7,39	-6,72	-0,32	-1,37	-4,72	-1,32	2,03
	B	75	72,78	-2,37	-2,78	64,40	15,00	-8,39	72,35	71,69	-7,96	-7,29	-0,41	-1,37	-4,72	-1,41	1,94
Thoracosphaera heimii	A	unmodified	0,69	-0,02	-5,71	-0,51	15,00	-1,20	0,26	1,33	-0,77	-1,84	-5,69	0,98	-2,36	-6,69	-3,35
	B	unmodified	0,69	-0,02	-5,65	-0,94	15,00	-1,63	0,26	1,33	-1,21	-2,28	-5,63	0,98	-2,36	-6,63	-3,29
	A	1	1,07	-0,03	-5,64	-0,43	15,00	-1,50	0,64	1,70	-1,07	-2,13	-5,61	0,97	-2,38	-6,61	-3,27
	B	1	1,07	-0,03	-5,80	-0,48	15,00	-1,55	0,64	1,70	-1,13	-2,19	-5,77	0,97	-2,38	-6,77	-3,43
	A	2	1,77	-0,06	-5,76	-0,09	15,00	-1,86	1,34	2,39	-1,43	-2,48	-5,70	0,94	-2,40	-6,70	-3,36
	B	2	1,77	-0,06	-5,69	-0,03	15,00	-1,80	1,34	2,39	-1,37	-2,41	-5,63	0,94	-2,40	-6,63	-3,29
	A	3	2,3	-0,07	-5,84	0,34	15,00	-1,96	1,87	2,91	-1,54	-2,57	-5,77	0,93	-2,42	-6,77	-3,43
	B	3	2,3	-0,07	-5,65	0,38	15,00	-1,92	1,87	2,91	-1,49	-2,52	-5,58	0,93	-2,42	-6,58	-3,24
	A	5	3,91	-0,13	-5,67	1,80	15,00	-2,11	3,48	4,48	-1,69	-2,68	-5,54	0,87	-2,47	-6,54	-3,20
	B	5	3,91	-0,13	-5,75	1,88	15,00	-2,03	3,48	4,48	-1,60	-2,60	-5,62	0,87	-2,47	-6,62	-3,28
	A	7	6,22	-0,20	-5,38	3,78	15,00	-2,44	5,79	6,73	-2,02	-2,95	-5,18	0,80	-2,55	-6,18	-2,84
	B	7	6,22	-0,20	-5,66	4,19	15,00	-2,03	5,79	6,73	-1,61	-2,54	-5,46	0,80	-2,55	-6,46	-3,11
	A	10	11,68	-0,38	-5,88	8,40	15,00	-3,28	11,25	12,06	-2,86	-3,66	-5,50	0,62	-2,72	-6,50	-3,16
	B	10	11,68	-0,38	-5,88	8,82	15,00	-2,86	11,25	12,06	-2,43	-3,24	-5,50	0,62	-2,72	-6,50	-3,16
	A	25	24,97	-0,81	-6,37	19,59	15,00	-5,38	24,54	25,03	-4,95	-5,44	-5,56	0,19	-3,16	-6,56	-3,22
	B	25	24,97	-0,81	-6,26	21,34	15,00	-3,63	24,54	25,03	-3,21	-3,69	-5,45	0,19	-3,16	-6,45	-3,10
	A	50	49,44	-1,61	-6,76	39,95	15,00	-9,49	49,01	48,91	-9,06	-8,95	-5,15	-0,61	-3,95	-6,15	-2,80
	B	50	49,44	-1,61	-6,81	42,01	15,00	-7,43	49,01	48,91	-7,00	-6,90	-5,20	-0,61	-3,95	-6,20	-2,86
	A	75	72,78	-2,37	-7,56	63,21	15,00	-9,57	72,35	71,69	-9,15	-8,48	-5,19	-1,37	-4,72	-6,19	-2,85
	B	75	72,78	-2,37	-7,58	62,45	15,00	-10,33	72,35	71,69	-9,91	-9,24	-5,21	-1,37	-4,72	-6,21	-2,87
Calcidiscus leptoporus	A	unmodified	0,69	-0,02	-2,32	-1,07	15,00	-1,76	0,26	1,33	-1,33	-2,40	-2,30	0,98	-2,36	-3,30	0,05
	B	unmodified	0,69	-0,02	-2,37	-1,02	15,00	-1,71	0,26	1,33	-1,29	-2,36	-2,35	0,98	-2,36	-3,35	-0,01
	A	1	1,07	-0,03	-1,59	-0,94	15,00	-2,01	0,64	1,70	-1,58	-2,64	-1,56	0,97	-2,38	-2,56	0,78
	B	1	1,07	-0,03	-2,78	-0,83	15,00	-1,90	0,64	1,70	-1,47	-2,53	-2,75	0,97	-2,38	-3,75	-0,40
	A	2	1,77	-0,06	-2,66	-0,34	15,00	-2,11	1,34	2,39	-1,69	-2,73	-2,60	0,94	-2,40	-3,60	-0,26
	B	2	1,77	-0,06	-2,71	-0,32	15,00	-2,09	1,34	2,39	-1,66	-2,71	-2,65	0,94	-2,40	-3,65	-0,31
	A	3	2,3	-0,07	-2,63	0,21	15,00	-2,09	1,87	2,91	-1,66	-2,69	-2,56	0,93	-2,42	-3,56	-0,21
	B	3	2,3	-0,07	-2,83	0,21	15,00	-2,09	1,87	2,91	-1,67	-2,70	-2,76	0,93	-2,42	-3,76	-0,41
	A	5	3,91	-0,13	-2,11	1,44	15,00	-2,47	3,48	4,48	-2,05	-3,04	-1,98	0,87	-2,47	-2,98	0,36
	B	5	3,91	-0,13	-3,08	1,54	15,00	-2,37	3,48	4,48	-1,95	-2,94	-2,95	0,87	-2,47	-3,95	-0,61
	A	7	6,22	-0,20	-3,59	3,43	15,00	-2,79	5,79	6,73	-2,37	-3,30	-3,39	0,80	-2,55	-4,39	-1,05
	B	7	6,22	-0,20	-3,49	3,46	15,00	-2,76	5,79	6,73	-2,33	-3,27	-3,29	0,80	-2,55	-4,29	-0,94
	A	10	11,68	-0,38	-2,92	8,14	15,00	-3,54	11,25	12,06	-3,12	-3,92	-2,54	0,62	-2,72	-3,54	-0,20
	B	10	11,68	-0,38	-2,94	8,23	15,00	-3,45	11,25	12,06	-3,02	-3,83	-2,56	0,62	-2,72	-3,56	-0,22
	A	25	24,97	-0,81	-3,79	18,44	15,00	-6,53	24,54	25,03	-6,10	-6,59	-2,98	0,19	-3,16	-3,98	-0,63
	B	25	24,97	-0,81	-3,91	19,10	15,00	-5,87	24,54	25,03	-5,45	-5,93	-3,10	0,19	-3,16	-4,10	-0,76
	A	50	49,44	-1,61	-4,10	40,97	15,00	-8,47	49,01	48,91	-8,04	-7,93	-2,49	-0,61	-3,95	-3,49	-0,14
	B	50	49,44	-1,61	-4,15	41,23	15,00	-8,21	49,01	48,91	-7,78	-7,68	-2,54	-0,61	-3,95	-3,54	-0,20
	A	75	72,78	-2,37	-4,79	56,70	15,00	-16,08	72,35	71,69	-15,66	-14,99	-2,42	-1,37	-4,72	-3,42	-0,08
	B	75	72,78	-2,37	-4,93	57,46	15,00	-15,32	72,35	71,69	-14,89	-14,22	-2,56	-1,37	-4,72	-3,56	-0,21

Table 4

	Previously-reported Vital Effect			Vital Effect (this study)	
Species Name	$\delta^{18}O_c - \delta^{18}O_{eq}$	factors for *p*H 8.2	Source	$\delta^{18}O_c - \delta^{18}O_{eq}$	$\delta^{13}C_c - \delta^{13}C_{DIC}$
Gephyrocapsa oceanica	2 2.5	2.4 2.9	Dudley et al. (1986) Ziveri et al. (2003)	1.3	0.3
Emiliania huxleyi	2.8 3.1	3.2 3.5	Dudley et al. (1986) Ziveri et al. (2003)	2.6	1
Coccolithus braarudii	1.7 -0.4	2.1 -0.4	Ziveri et al. (2003) Stevenson et al. (2014)	-0.2	-1.6
Thoracosphaera heimii	-3.1	-2.8	Zonneveld et al. (2007)	-1	-6.7
Calcidiscus leptoporus	-2.4 -0.2 -1.1	-2 0.2 -1.1	Dudley et al. (1986) Ziveri et al. (2003) Candelier et al. (2013)	-1.3	-3.3